iScience

CellPress
OPEN ACCESS

Article

GhPIPLC2D promotes cotton fiber elongation by enhancing ethylene biosynthesis

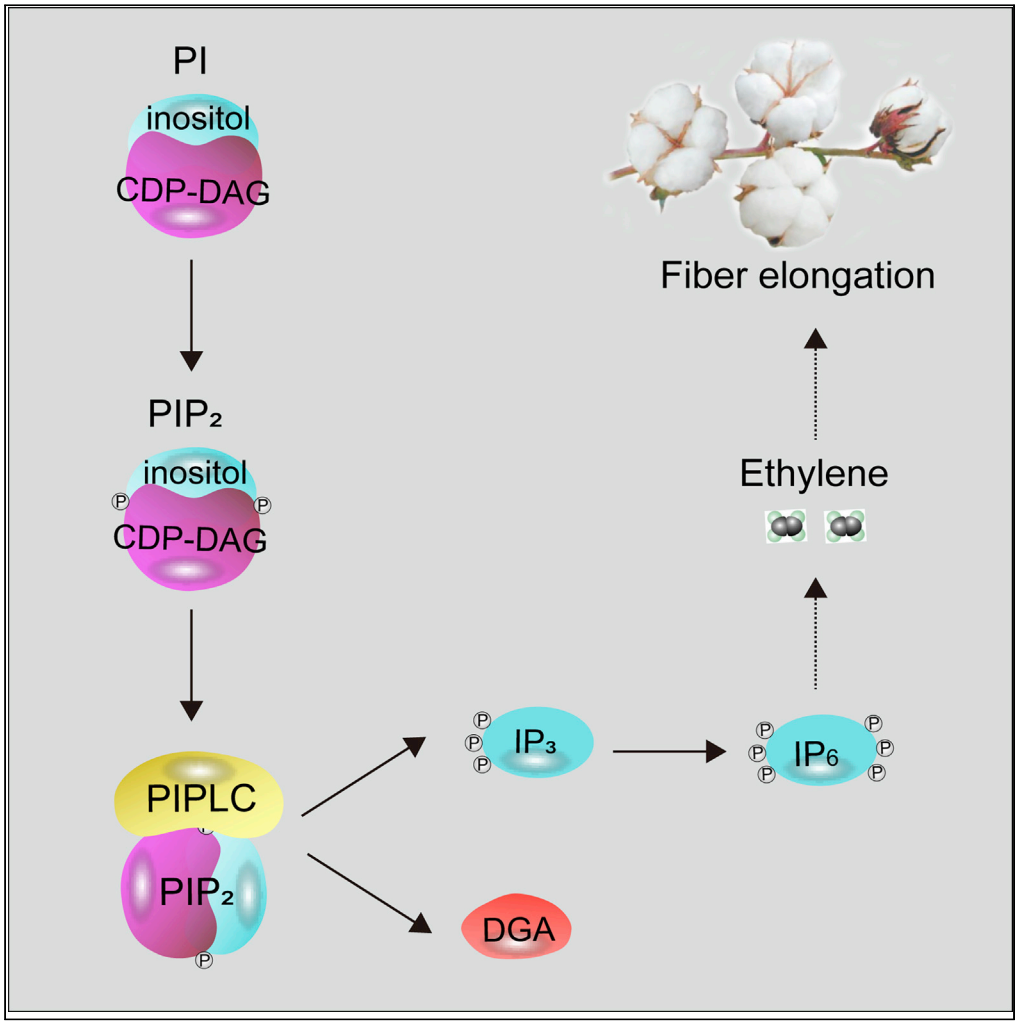

Liping Zhu, Lingling Dou, Haihong Shang, Hongbin Li, Jianing Yu, Guanghui Xiao

lihb@shzu.edu.cn (H.L.)
jnyu@snnu.edu.cn (J.Y.)
guanghuix@snnu.edu.cn (G.X.)

HIGHLIGHTS

GhPIPLC2D positively regulates cotton fiber elongation

GhPIPLC2D cleaves PIP_2 into IP_3, which could be phosphorylated to IP_6

IP_6 enhances fiber elongation via improving ethylene biosynthesis

Zhu et al., iScience *24*, 102199
March 19, 2021
https://doi.org/10.1016/j.isci.2021.102199

iScience

CellPress
OPEN ACCESS

Article

GhPIPLC2D promotes cotton fiber elongation by enhancing ethylene biosynthesis

Liping Zhu,[1] Lingling Dou,[2] Haihong Shang,[3] Hongbin Li,[4,*] Jianing Yu,[1,*] and Guanghui Xiao[1,5,*]

SUMMARY

Inositol-1,4,5-trisphosphate (IP_3) is an important second messenger and one of the products of phosphoinositide-specific phospholipase C (PIPLC)-mediated phosphatidylinositol (4,5) bisphosphate (PIP_2) hydrolysis. However, the function of IP_3 in cotton is unknown. Here, we characterized the function of *GhPIPLC2D* in cotton fiber elongation. *GhPIPLC2D* was preferentially expressed in elongating fibers. Suppression of *GhPIPLC2D* transcripts resulted in shorter fibers and decreased IP_3 accumulation and ethylene biosynthesis. Exogenous application of linolenic acid (C18:3) and phosphatidylinositol (PI), the precursor of IP_3, improved IP_3 and myo-inositol-1,2,3,4,5,6-hexakisphosphate (IP_6) accumulation, as well as ethylene biosynthesis. Moreover, fiber length in *GhPIPLC2D*-silenced plant was reduced after exogenous application of IP_6 and ethylene. These results indicate that *GhPIPLC2D* positively regulates fiber elongation and IP_3 promotes fiber elongation by enhancing ethylene biosynthesis. Our study broadens our understanding of the function of IP_3 in cotton fiber elongation and highlights the possibility of cultivating better cotton varieties by manipulating *GhPIPLC2D* in the future.

INTRODUCTION

Inositol-1,4,5-trisphosphate (IP_3) and diacylglycerol (DAG) are two important second messengers that convert extracellular signals to intracellular signals in plants (Singh et al., 2015). Phosphoinositide-specific phospholipase C (PIPLC) catalysis of the substrate phosphatidylinositol (4,5) bisphosphate (PIP_2) produces both messenger molecules (Abd-El-Haliem and Joosten, 2017). Reversible inactivation of guard cell K^+ channels is controlled by cytoplasmic Ca^{2+} that rely on IP_3 signal cascades (Blatt et al., 1990). In tomato plants, reduction of IP_3 content modifies the inositol phosphate pathway and affects light signaling and secondary metabolism (Alimohammadi et al., 2012). IP_3 suppresses protein degradation in plant vacuoles by regulating sorting nexin-mediated protein sorting (Chu et al., 2016). In post-harvest peach fruit, IP_3 is also involved in nitric oxide-enhanced chilling tolerance and defense response (Jiao et al., 2019).

When phosphorylated, IP_3 forms inositol hexaphosphate (Dong et al., 2019), which has many functions in plants. Also known as phytic acid, IP_6 is the main form of storage of phosphorus in mature seeds (Gibson et al., 2018). Inositol hexaphosphate can stimulate Ca^{2+} release to participate in many signaling pathways (Lee et al., 2015). As an endomembrane-acting Ca^{2+} release signal, IP_6 activates both fast and slow conductance of the guard cell vacuole (Lemtiri-Chlieh et al., 2003). In plant hormone perception, IP_6 can bind to the auxin receptor complex TIR1/IAA (Tan et al., 2007). Gibberellic acid has been shown to affect the degradation of IP_6 in soybean sprouts with the calcium transport (Hui et al., 2018).

Phosphatidylinositol (PI), the precursor of IP_3, is composed of 1,2-DAG phosphate and inositol. As the major phospholipid in cell membranes, PI plays critical roles in various physiological processes in plants (Hänninen et al., 2017; Heilmann, 2016). Phosphorylation of PI produces phosphatidylinositol 4-phosphate (PIP_4) of which can be further catalyzed to generate PIP_2 (Munnik and Nielsen, 2011), a kind of membrane phospholipid involved in various developmental stages in plants (Shimada et al., 2019; Kusano et al., 2008). Mitogen-activated protein kinase 6 (MPK6)-mediated phosphorylation of PI 4-phosphate 5-kinase 6 limits the production of the pool of functional PIP_2 in response to the pathogen-associated molecular pattern-triggered immunity in *Arabidopsis thaliana* (Menzel et al., 2019). Directional growth is regulated by

[1]College of Life Sciences, Shaanxi Normal University, Xi'an 710119, China

[2]School of Chemistry and Chemical Engineering, Xianyang Normal University, Xianyang 712000, China

[3]Zhengzhou Research Base, State Key Laboratory of Cotton Biology, Zhengzhou University, Zhengzhou 450000, China

[4]College of Life Sciences, Key Laboratory of Xinjiang Phytomedicine Resource and Utilization of Ministry of Education, Shihezi University, Shihezi 832003, China

[5]Lead contact

*Correspondence: lihb@shzu.edu.cn (H.L.), jnyu@snnu.edu.cn (J.Y.), guanghuix@snnu.edu.cn (G.X.)

https://doi.org/10.1016/j.isci.2021.102199

MPK6 controlling PIP_2 production and membrane trafficking in pollen tubes in *Arabidopsis* (Hempel et al., 2017). *Arabidopsis* plasma membrane-associated Ca^{2+}-binding protein 2 regulates PIP_2 in membranes to attenuate root hair elongation (Kato et al., 2019).

PIPLC, an important lipid hydrolase in plants, cleaves PIP_2 into two important secondary messengers, IP_3 and DAG (Mueller-Roeber and Pical, 2002; Kadamur and Ross, 2013). The four conserved domains of PIPLC are named EF-hand, PI-PLC-X, PI-PLC-Y, and C2 (Zhang et al., 2018a). The EF-hand domain consists of two helix-loop-helix folding motifs for calcium-binding. The catalytic activity of all PIPLCs is strictly dependent on the PI-PLC-X and PI-PLC-Y domains. The C2 domain has been identified in all plant PIPLCs and functions along with the participation of calcium, in binding phospholipids (Pokotylo et al., 2014). The PIPLC plays multiple roles in plant stress response and development.

There are nine *AtPIPLC* genes in *Arabidopsis* (Tasma et al., 2008). *AtPIPLC2* is required for seedling growth (Di Fino et al., 2017) and *AtPIPLC5* is involved in primary and secondary root growth (Zhang et al., 2018c). *AtPIPLC3* and *AtPIPLC9* play critical roles in thermo-tolerance response (Gao et al., 2014; Zheng et al., 2012). *AtPIPLC4* is up-regulated after salt stimulation (Tasma et al., 2008). In addition, overexpression of *AtPIPLC5* and *AtPIPLC7* improves plant drought tolerance (Zhang et al., 2018c; Van Wijk et al., 2018). *AtPIPLC2*-silenced plants are more susceptible to bacterial and fungal infections, suggesting that *AtPIPLC2* is involved in plant immune response (D'Ambrosio et al., 2017).

Cotton fiber is an important industrial textile material in the world (Li et al., 2015). Fuzz and lint are two types of cotton fibers. Fuzz fibers only grow to a maximum length of 5 mm after seed maturity which cannot be used in textile (Arpat et al., 2004). Lint fibers develop into sufficiently long fibers desired for textile products (Kim and Triplett, 2001). The *fuzzless* and *lintness* mutant (*fl*) has been widely used to investigate the developmental mechanism of cotton fibers (Wu et al., 2017; Hu et al., 2018). Multiple genes are reported to be involved in cotton fiber development, including genes related to phytohormones (Xiao et al., 2019; Zhang et al., 2011), plant growth and development (Zhang et al., 2018a), and biotic and abiotic stress responses (He et al., 2019). Linolenic acid (C18:3) enhanced cotton fiber elongation by improving PI and phosphatidylinositol monophosphate biosynthesis (Liu et al., 2015). The promoter of *FLORAL BINDING PROTEIN 7* (*FBP7*) drives the *iaaM* gene expression in the cotton ovule epidermis at the fiber initiation stage, which increased IAA levels and enhanced the number of lint fibers (Zhang et al., 2011). Exogenous GA3 increases fiber length via regulating *cellulose synthase* (*CesA*) gene expression, because of the GA-responsive elements present in the promoters of several *CesA* genes (Xiao et al., 2016). A cotton NAC transcription factor (*FSN*) that acts a master switch in regulating secondary cell wall development, activates its downstream secondary cell wall-related genes to promote cotton fiber development (Zhang et al., 2018b). *GhCFE1A* plays a critical role in fiber cell initiation and elongation during cotton fiber development and likely functions as a dynamic link between the actin cytoskeleton and endoplasmic reticulum (ER) network (Lv et al., 2015).

Ethylene, one of the major hormones in plants, participates in cotton fiber development (Li et al., 2007; Qin et al., 2007; Shi et al., 2003, 2006). The transcripts of three ethylene biosynthesis genes 1-aminocyclopropane-1-carboxylic acid oxidases (*GhACO1-3*) were highly accumulated at the fiber elongation stage. Exogenous application of ethylene promotes fiber elongation, as evidenced by an *in vitro* application of an ethylene-synthesis inhibitor, L-(2-aminoethoxyvinyl)-glycine, that hindered cotton fiber elongation (Shi et al., 2003, 2006). Ethylene may also promote fiber elongation by enhancing H_2O_2 production, which in turn induces ascorbate peroxidase activity (GhAPX1) in cotton fibers. The high expression of *GhAPX1* observed in wild-type (WT) cotton fibers and little to no expression of *GhAPX1* observed in *fuzzless-lintness* (*fl*) mutant ovules suggest an important role of *GhAPX1* in fiber development (Li et al., 2007). Lignoceric acid can also enhance fiber cell elongation by increasing ethylene biosynthesis. Moreover, ethylene can eliminate the inhibition of fiber cell elongation caused by application of 2-chloro-N-[ethoxymethyl]-N-[2-ethyl-6-methyl-phenyl]-acetamide, an inhibitor of the biosynthesis of very-long-chain fatty acids (Qin et al., 2007).

In this work, we found that the expression level of *GhPIPLC2D* was significantly upregulated in the cotton fiber elongation stage and IP_3 accumulation was much higher in WT fibers compared to that in WT and *fl* ovules at 10 days post-anthesis (DPA). Furthermore, silencing *GhPIPLC2D* reduced fiber length, IP_3 accumulation and ethylene content. Exogenous application of linolenic acid and PI, the precursor of PIP_2, improved IP_3 and IP_6 contents as well as ethylene biosynthesis. Exogenous application of IP_6, the phosphorylation product of IP_3, also significantly enhanced ethylene biosynthesis. These results indicate that

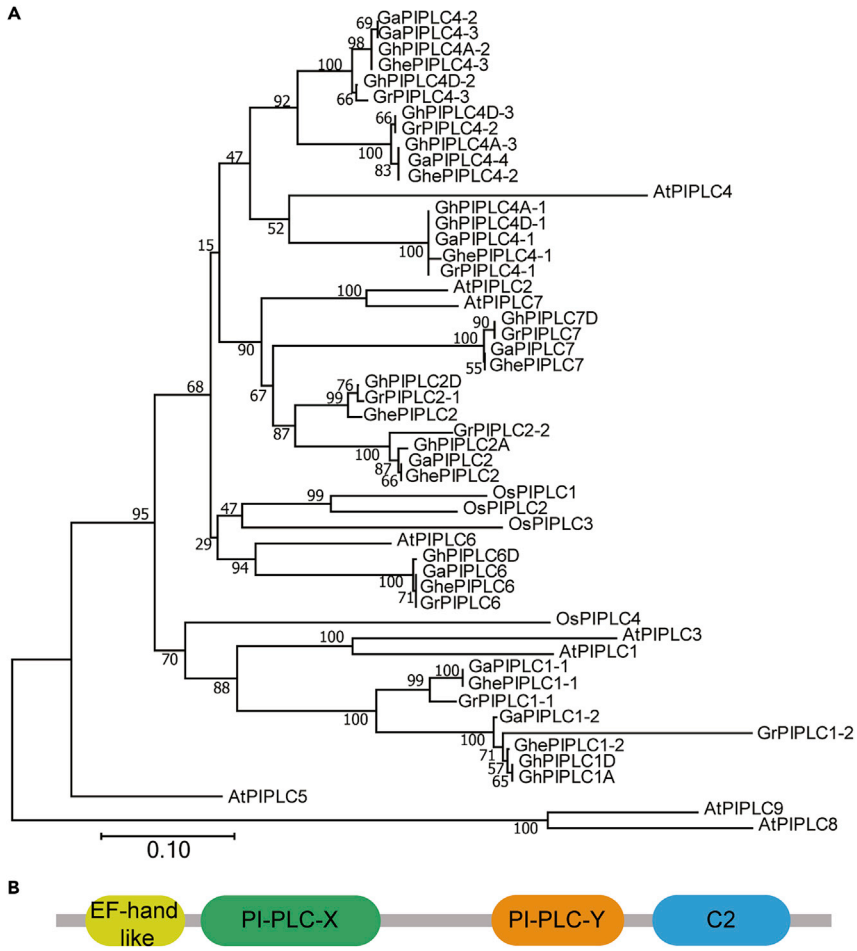

Figure 1. Phylogenetic analysis and conserved domains of GhPIPLCs

(A) phylogenetic analysis of 12 GhPIPLCs, 9 GaPIPLCs, 9 GrPIPLCs, 9 GhePIPLCs, 9 AtPIPLCs, and 4 OsPIPLCs. Numbers indicate bootstrap confidence percentages. Scale indicates evolutionary distance.

(B) conserved domains of GhPIPLCs. The gray line indicates protein sequence length. Boxes with different colors represent different conserved domains of the GhPIPLC proteins.

GhPIPLC2D promotes cotton fiber elongation by increasing IP_3 accumulation, which in turn stimulates ethylene biosynthesis.

RESULTS

Conserved domains and phylogenetic analysis of GhPIPLCs

In plants, PIPLCs are structurally composed of four conserved domains, the EF-hand-like, PI-PLC-X, PI-PLC-Y, and C2 domains (Abd-El-Haliem and Joosten, 2017). Amino acid sequences of 12 GhPIPLCs were obtained from a previous study (Zhang et al., 2018a). Here, we renamed the GhPIPLCs according to the phylogenetic relationships of GhPIPLCs and AtPIPLCs (Figure 1A); the names and corresponding genome IDs of GhPIPLCs are shown in Table S1. To investigate the sequence conservation of GhPIPLCs, all GhPIPLC members were submitted for analysis by the Pfam online tools (http://pfam.xfam.org/) to obtain more detailed conserved domain information. All GhPIPLCs possessed four domains (Figure 1B) with the exceptions of GhPIPLC1A, GhPIPLC1D, and GhPIPLC6D, which lacked the EF-hand-like domain (Figure S1), indicating that these three GhPIPLCs may be functionally more diverse than the GhPIPLCs that contain all four domains.

In order to explore the evolutionary relationships of PIPLCs, the protein sequences of PIPLCs from *G. hirsutum*, *A. thaliana*, *G. arboreum*, *G. raimondii*, *G. herbaceum*, and *Oryza sativa* were obtained to generate a rooted phylogenetic tree. As shown in Figure 1, GhPIPLC1A and GhPIPLC1D had the longest

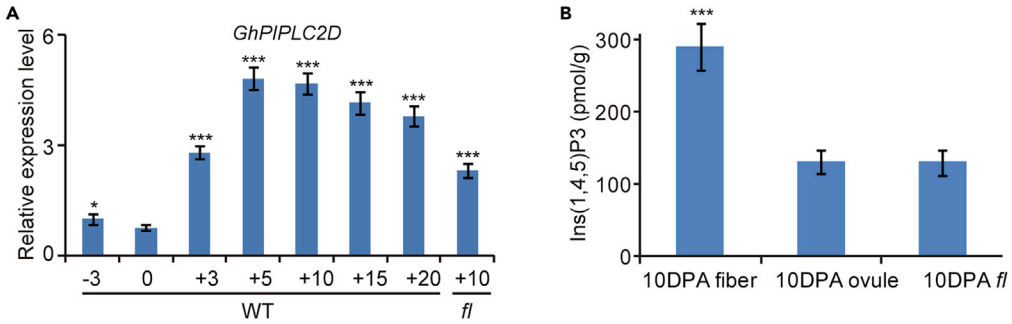

Figure 2. Expression of the *GhPIPLC2D* gene and IP_3 accumulation in cotton fibers and ovules

(A) the expression levels of *GhPIPLC2D* during fiber development between 3 day prior to anthesis to 20 days post-anthesis. Gene expression data were obtained by quantitative real-time PCR with three independent replicates. Error bars represent the SE (n = 3 biological replicates). Statistical significance was determined using one-way ANOVA with Tukey's test.

(B) analysis of IP_3 accumulation in fibers, WT ovules and *fl* ovules 10 DPA. Statistical significance was determined using one-way ANOVA with Tukey's test. Error bars represent the SE (n = 3 biological replicates). *p < 0.05, ***p < 0.001. WT, wild-type; *fl*, *fuzzless-lintless* mutant; DPA, days post-anthesis.

evolutionary distances compared with the distances of other GhPIPLCs. There were six GhPIPLCs (GhPIPLC4A-3, GhPIPLC4D-3, GhPIPLC4A-2, GhPIPLC4D-2, GhPIPLC4A-1, and GhPIPLC4D-1), four GaPIPLCs (GaPIPLC4-1, GaPIPLC4-2, GaPIPLC4-3, GaPIPLC4-4), three GhePIPLCs (GhePIPLC4-1, GhePIPLC4-2, GhePIPLC4-3), three GrPIPLCs (GrPIPLC4-1, GrPIPLC4-2, GrPIPLC4-3) and one AtPIPLC4 in the same branch, indicating that GhPIPLC4 may extensively expand in *Gossypium*. To explore the potential driving force of PIPLC4 expansion, we analyzed duplication events in the *PIPLC* genes and found that tandem duplication is the main contributor to the expansion of *PIPLC4* genes in *Gossypium* (Table S2).

GhPIPLC and IP_3 are associated with cotton fiber elongation

To investigate the potential functions of *GhPIPLC* genes in cotton, the expression profiles of individual members of *GhPIPLCs* in cotton fiber and ovules were obtained from CottonFDG (https://cottonfgd.org/) and examined over developmental time from 5 to 25 DPA. The results showed that six members of *GhPIPLCs* (*GhPIPLC4A-2*, *GhPIPLC4D-2*, *GhPIPLC4A-3*, *GhPIPLC4D-3*, *GhPIPLC2A*, and *GhPIPLC2D*) were predominantly expressed during cotton fiber development. Notably, *GhPIPLC2A* and *GhPIPLC2D* had the highest and similar expression patterns in the fiber elongation stage (Figure S2), suggesting these two genes might have similar contributions to cotton fiber development. *GhPIPLC2A* and *GhPIPLC2D* were likely homoeologous genes with 84.94% similarity in coding sequences. Therefore, we amplified *GhPIPLC2D* and checked the sequence specificity via clone sequencing for subsequent functional analyses. The results showed that the *GhPIPLC2D* coding sequence, but not the *GhPIPLC2A* coding sequence, was successfully amplified. The expression levels of *GhPIPLC2D* in different cotton fiber development stages were further confirmed using quantitative real-time polymerase chain reaction (qRT-PCR). As shown in Figure 2A, the expression level of *GhPIPLC2D* was significantly higher in the fiber elongation stage with peak levels occurring at 5 and 10 DPA than at prior sampling times (Figure 2A), implying the *GhPIPLC2D* gene may play a critical role in cotton fiber elongation. Furthermore, we detected content of IP_3, one of the catalytic products of PIPLC, in fibers and ovules 10 DPA from Xuzhou-142 WT and mutant *fl* plants and found that IP_3 content was higher in 10 DPA WT fibers than that in 10 DPA WT and *fl* ovules (Figure 2B). Taken together, these results suggest that *GhPIPLC2D* may promote cotton fiber cell development by regulating IP_3 accumulation.

Silencing *GhPIPLC2D* in cotton inhibits fiber elongation

To better understand the biological function of *GhPIPLC2D* in cotton fiber development, *GhPIPLC2D* was silenced in *G. hirsutum* using the virus-induced gene silencing (VIGS) strategy. Our results show that the expression level of *GhPIPLC2D* was clearly reduced in *GhPIPLC2D*-silenced cotton plants in contrast to the control plants (Figure 3A). We also analyzed the expression of *GhPIPLC2A* gene in *GhPIPLC2D*-silenced plants and the results show that *GhPIPLC2A* transcripts in *GhPIPLC2D*-silenced plants were similar to the control plants, indicating that *GhPIPLC2A* transcripts are not decreased in *GhPIPLC2D*-silenced plants

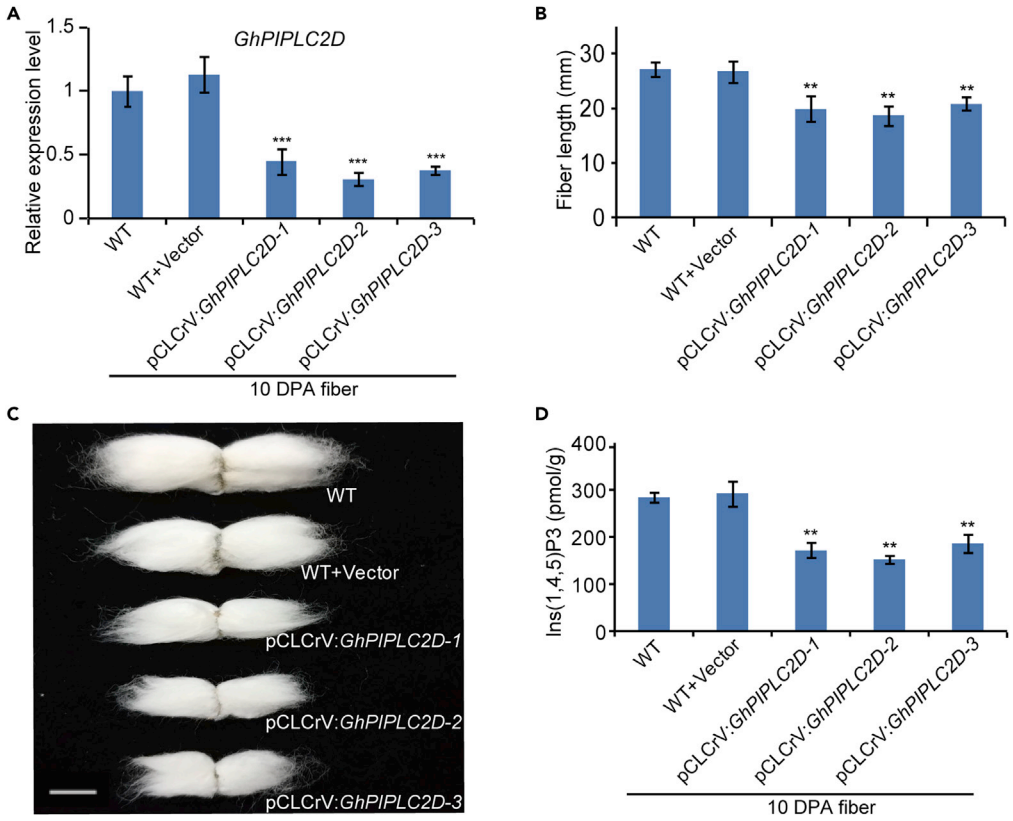

Figure 3. *GhPIPLC2D* is involved in cotton fiber elongation

(A) the expression levels of *GhPIPLC2D* in fibers of WT and *GhPIPLC2D*-silenced plants 10 DPA. Gene expression data were obtained by quantitative real-time PCR with three independent replicates.

(B) comparison of fiber lengths in WT and *GhPIPLC2D*-silenced plants.

(C) representative seeds with attached fibers from the VIGS experiment. Scale bar = 1 cm.

(D) comparison analysis of IP_3 contents in WT and *GhPIPLC2D*-silenced plants. Statistical significance was determined using one-way ANOVA with Tukey's test. Error bars represent the SE (n = 3 biological replicates). $^{**}p < 0.01$, $^{***}p < 0.001$. WT, wild-type.

(Figure S3). We further measured the lengths of mature fibers in *GhPIPLC2D*-silenced and control plants. *GhPIPLC2D*-silenced plants displayed shorter fiber length than that in control plants (Figures 3B and 3C). In addition, suppression of *GhPIPLC2D* expression significantly reduced IP_3 accumulation in 10 DPA fiber cells (Figure 3D). These observations are additional evidence of *GhPIPLC2D* possibly regulating IP_3 accumulation, which is essential for cotton fiber cell development.

GhPIPLC2D gene promotes cotton fiber growth by regulating ethylene biosynthesis

A previous study demonstrated that ethylene plays a key role in promoting cotton fiber elongation and the 1-aminocyclopropane-1-carboxylic acid oxidase1 (*ACO1*) and *ACO3* genes, two key genes for ethylene biosynthesis, were highly expressed during the fiber growth stage (Shi et al., 2003, 2006). In order to explore the molecular mechanism of *GhPIPLC2D* in regulating fiber growth, we detected the expression of the *GhACO1* and *GhACO3* genes as well as ethylene accumulation in *GhPIPLC2D*-silenced and non-silenced plants. Our results show that the expression of *GhACO1* and *GhACO3* were significantly down-regulated in *GhPIPLC2D*-silenced cotton when compared with non-silenced cotton (Figures 4A and 4B).

We also detected ethylene production in *GhPIPLC2D*-silenced and non-silenced plants. As expected, the accumulation of ethylene was significantly lower in *GhPIPLC2D*-silenced cotton (Figure 4C). Ethylene accumulation in *GhPIPLC2D*-silenced plants was reduced to half of that in the non-silenced plants after six days in culture (Figure 4D). These results suggest that the *GhPIPLC2D* gene may promote cotton fiber

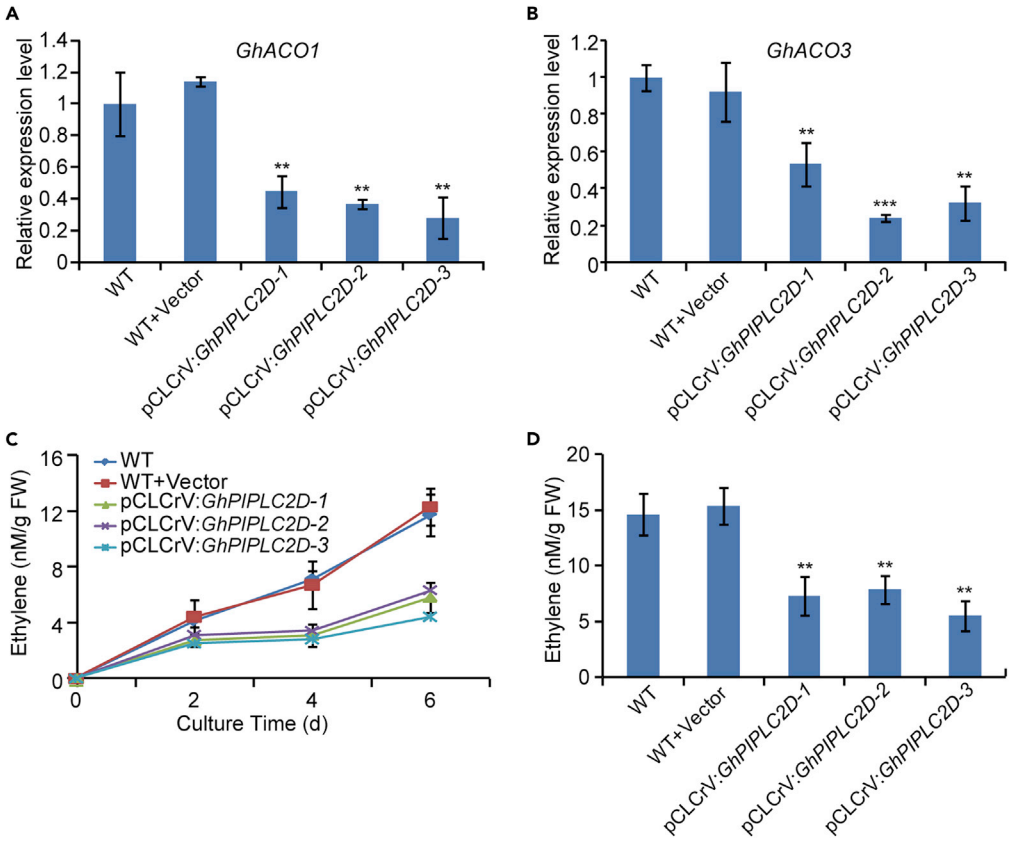

Figure 4. Silencing the *GhPIPLC2D* gene reduced ethylene biosynthesis and production

Relative expression levels of *GhAC O 1* (A) and *GhAC O 3* (B) in 10 DPA fibers of WT and *GhPIPLC2D*-silenced plants. Gene expression data were obtained by quantitative real-time PCR with three independent replicates. The relative expression level of each gene was determined after normalizing to the expression level of the WT, which was set to 1.0.

(C) ethylene production in 10 DPA fibers of WT and *GhPIPLC2D*-silenced plants.

(D) ethylene production from ovules of WT and *GhPIPLC2D*-silenced plants cultured for six days. Statistical significance was determined using one-way ANOVA with Tukey's test. Error bars represent the SE (n = 3 biological replicates). **p < 0.01, ***p < 0.001. WT, wild-type.

development by stimulating the expression of ethylene biosynthesis-related genes and ultimately enhance ethylene production.

Linolenic acid and PI increase IP_3 and IP_6 contents and ethylene biosynthesis

The synthetic precursor of PIP_2 and the catalytic substrate of PIPLC is PI, which is composed of phosphoric acid 1,2-DAG and inositol (Mueller-Roeber and Pical, 2002). Linolenic acid (C18:3) and palmitic acid (C16:0) were the most abundant fatty acids (FA) in PI from the 10 DPA fiber samples. The structural formula of PI biosynthesis is shown in Figure S4.

Carbenoxolone and 5-hydroxytryptamine inhibit the biosynthesis of C18:3 and PI, respectively (Liu et al., 2015). To better understand the effects of C18:3 and PI on cotton fiber cell growth, we detected the amounts of IP_3, IP_6, ethylene and expression of ethylene biosynthesis-related genes after exogenous applications of C18:3, PI, carbenoxolone and 5-hydroxytryptamine to 1 DPA cotton ovules for six days. The results revealed that exogenous application of each C18:3 and PI markedly improved IP_3 accumulation, whereas *in vitro* application of the corresponding inhibitors, carbenoxolone and 5-hydroxytryptamine, apparently reduced IP_3 accumulation (Figure 5A). The qRT-PCR experiment showed that ethylene biosynthesis-related genes *GhACO1* and *GhACO3* were significantly upregulated after C18:3 or PI application (Figure 5B). Furthermore, *in vitro* applications of C18:3 or PI significantly promoted ethylene accumulation,

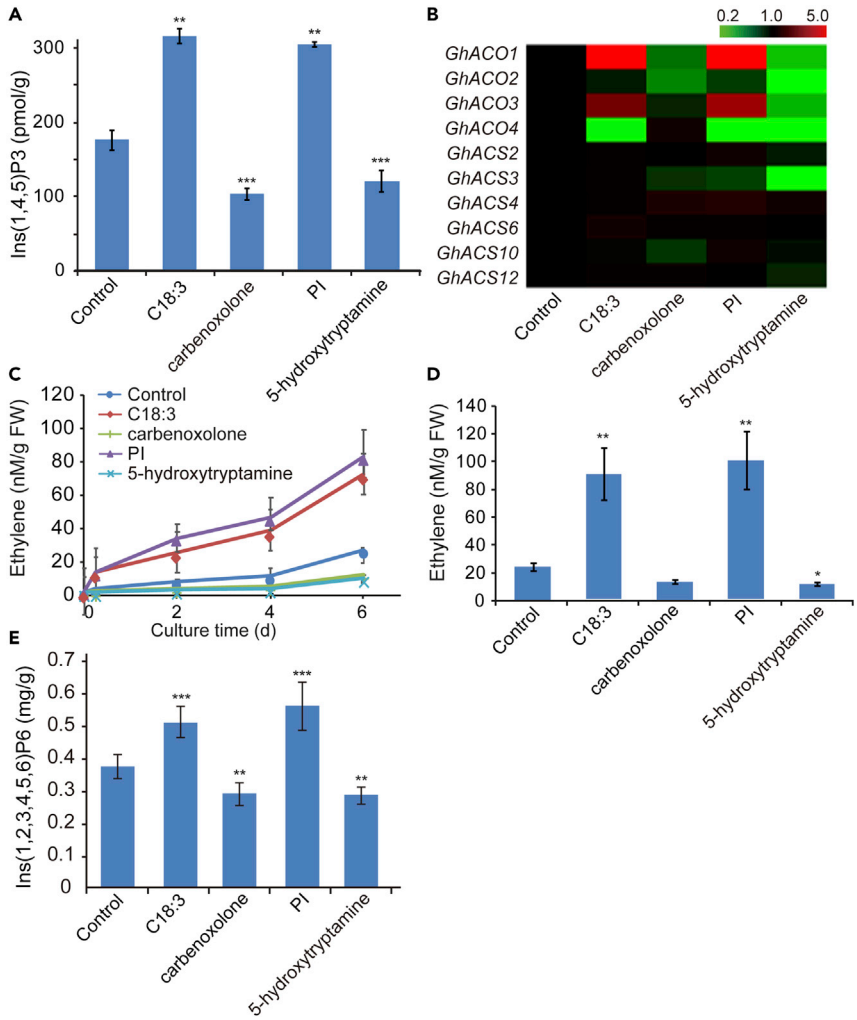

Figure 5. C18:3 and PI promote IP_3 and IP_6 production and ethylene biosynthesis

Accumulation of IP_3 (A) and ethylene biosynthesis gene transcripts (B) in ovules treated *in vitro* with C18:3, the C18:3 inhibitor carbenoxolone, PI or the PI inhibitor 5-hydroxytryptamine. Gene transcripts in (B) were obtained by qRT-PCR with three replicates.

(C) ethylene production in the same treatments as in (A).

(D) ethylene production over six days of ovule cultivation with the same treatments as in (A).

(E) IP_6 accumulation in ovules treated *in vitro* with C18:3, the C18:3 inhibitor carbenoxolone, PI or the PI inhibitor 5-hydroxytryptamine. *$p < 0.05$, **$p < 0.01$, ***$p < 0.001$. Statistical significance was determined using one-way ANOVA with Tukey's test. Error bars represent the SE (n = 3 biological replicates). No chemicals were added the control.

whereas their corresponding inhibitors dramatically inhibited ethylene production (Figure 5C). After C18:3 or PI treatment for six days, ethylene accumulation nearly increased four times that of the control group. However, the corresponding inhibitor-treated samples decreased ethylene production to half of that of the control (Figure 5D). Meanwhile, although IP_6 have higher content in ovules, the IP_6 content was increased from 0 DPA and reached a peak at 20 DPA during fiber development (Figure S5), and IP_6 accumulation was significantly improved after C18:3 and PI treatments (Figure 5E). These results imply that C18:3 and PI promote IP_3 and IP_6 accumulation as well as ethylene biosynthesis.

The C18 fatty acid contains saturated fatty acid C18:0 and unsaturated fatty acids C18:1, C18:2, and C18:3 (Conte et al., 2018). To investigate whether other C18 fatty acids could stimulate IP_3 accumulation, the levels of IP_3 in ovules treated with C18:0, C18:1, C18:2, or C18:3 were measured. Exogenous application of C18:0, C18:1, and C18:2 did not increase IP_3 contents compared with that of the control; only *in vitro*

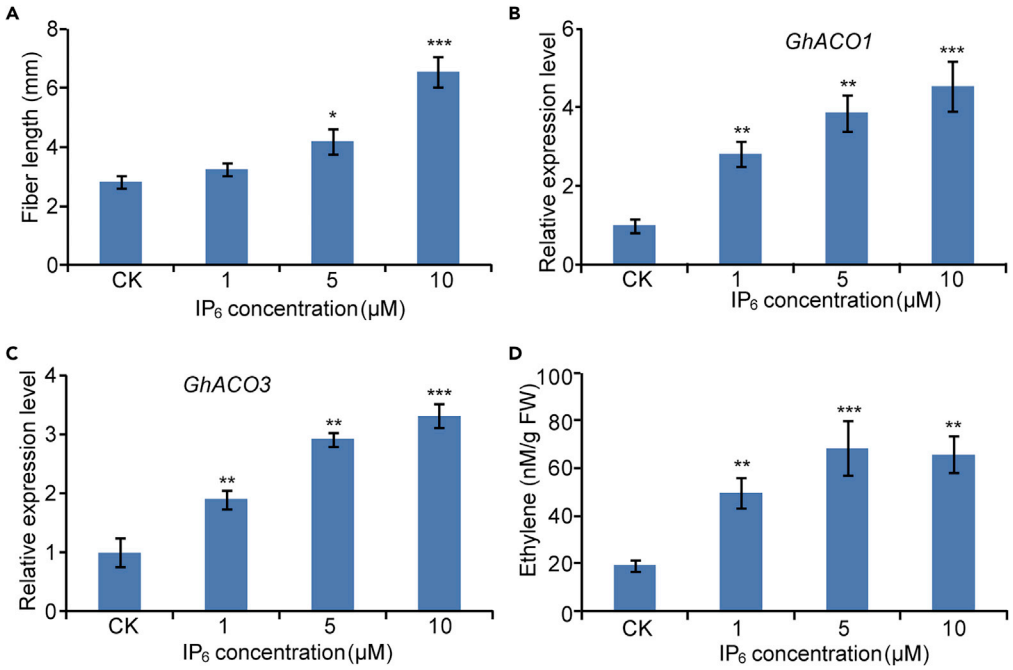

Figure 6. Fiber length and ethylene production increased after IP_6 treatment *in vitro*

Analysis of fiber length (A) and *GhAC O 1* (B) and *GhAC O 3* (C) gene expression, as well as ethylene production (D) after treatment with different concentrations of IP_6 *in vitro*. Relative expression levels of each gene were determined after normalizing to the expression level in the control, which was set to 1.0. Statistical significance was determined using one-way ANOVA with Tukey's test. Error bars represent the SE (n = 3 biological replicates). *p < 0.05, **p < 0.01, ***p < 0.001. No chemicals were added to the control.

application of C18:3 improved IP_3 accumulation (Figure S6). We further analyzed the total fatty acid signal intensities extracted from different tissues of cotton. The results showed that C16:0, C18:2, and C18:3 were the most abundant fatty acids in flowers, leaves, and ovules. Moreover, flowers, leaves, and ovules also contained higher amounts of total fatty acids than that from roots and stems (Figure S7).

IP_6 improves fiber length and ethylene biosynthesis

Catalysis of PIP_2 by PIPLC produces IP_3, which can be further phosphorylated to form IP_6 (Gibson et al., 2018). In order to determine whether IP_6 potentially regulates cotton fiber elongation and ethylene biosynthesis, we measured cotton fiber length, ethylene biosynthesis-related gene expression and the amount of ethylene accumulation in response to different concentrations of IP_6 treatment. We observed an increase of fiber length in a dose-dependent manner with the increase of IP_6 concentrations from 1 to 10 μM (Figure 6A). Fiber length increased three-fold that of the control group after treatment with 10 μM IP_6. Furthermore, exogenous application of IP_6 increased the expression of *GhACO1* (Figure 6B) and *GhACO3* (Figure 6C). As expected, ethylene accumulation (Figure 6D) also increased after IP_6 treatment *in vitro*. These results suggest that IP_6 can promote fiber elongation and ethylene biosynthesis.

Ethylene and IP_6 significantly promoted fiber cell elongation in *GhPIPLC2D*-silenced cotton

To further understand the biological role of IP_6 and ethylene on cotton fiber cell development, WT and *GhPIPLC2D*-silenced cotton ovules collected at 1 DPA were cultured with 5 μM IP_6 and 0.01 μM ethylene for 6 days. Subsequently, the length of fiber cells was observed and measured in microscope. The result showed that exogenous application of ethylene and IP_6 significantly enhanced the fiber length of *GhPIPLC2D*-silenced cotton and WT (Figure 7A). Furthermore, the fiber length of *GhPIPLC2D*-silenced plants treated with ethylene and IP_6 was obviously longer than the samples without any treatment (Figure 7B). These results suggest that ethylene and IP_6 can recover fiber length shortened by *GhPIPLC2D* gene silencing.

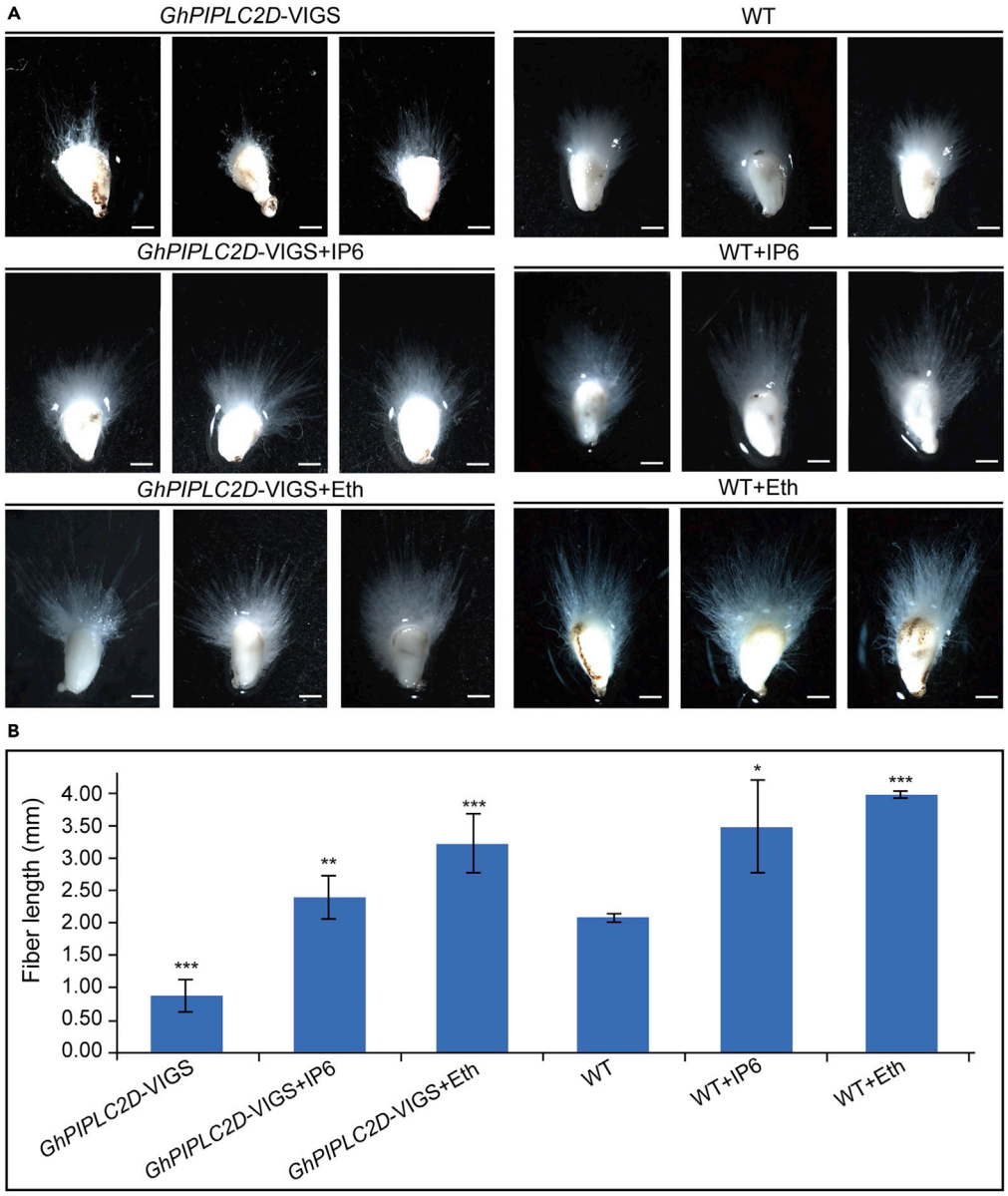

Figure 7. Exogenous application of ethylene and IP_6 promoted fiber length of *GhPIPLC2D*-silenced cotton

(A) phenotype of fiber cells from WT, *GhPIPLC2D*-silenced plant and WT, *GhPIPLC2D*-silenced plant with ethylene and IP_6 application, respectively. Scale bar = 2mm.

(B) comparison of fiber lengths in WT, *GhPIPLC2D*-silenced plants and WT, *GhPIPLC2D*-silenced plant with ethylene and IP_6 application, respectively. Statistical significance was determined using one-way ANOVA with Tukey's test. Error bars represent the SE (n = 3 biological replicates). $^{**}p < 0.01$, $^{***}p < 0.001$. WT, wild-type.

DISCUSSION

The PIPLC gene family contains nine members in *Arabidopsis* (Tasma et al., 2008), four members in rice (Singh et al., 2013) and twelve members in *G. hirsutum* (Zhang et al., 2018a). The PIPLC protein is usually composed of four conserved domains (Abd-El-Haliem and Joosten, 2017). In *G. hirsutum*, GhPIPLCs contained four conserved domains, except for GhPIPLC1A, GhPIPLC1D and GhPIPLC6D, which lacked the EF-hand-like domain (Figure S1). Interestingly, mutating an EF-hand-like domain of PIPLC did not affect Ca^{2+}-dependent substrate hydrolysis in *Dictyostelium discoideum* (Drayer et al., 1995), suggesting the domain may not be a regulatory site of the Ca^{2+} dependence of the PIPLC reaction, although the EF-hand-like domain is required for enzyme activity.

Phylogenetic analysis showed that six GhPIPLC4s, four GaPIPLC4s, three GhePIPLC4s, three GrPIPLC4s and one AtPIPLC4 were in the same evolutionary branch (Figure 1), indicating that the PIPLC4 sequence might have expanded in *Gossypium*. In *Arabidopsis*, the expression of *AtPIPLC4* is positively upregulated after salt stimulation (Tasma et al., 2008). OsPIPLC1 prefers to hydrolyze PIP_2 and elicits stress-induced Ca^{2+} signals to regulate salt tolerance (Li et al., 2017). Meanwhile, cotton is a moderately salt-tolerant crop with a salinity threshold level of 7.7 dS m^{-1} and has a higher basal level of tolerance to NaCl compared to that of other major crops (Sharif et al., 2019), Li et al., 2015). The moderate level of salt tolerance implies that *GhPIPLC4A-1*, *GhPIPLC4D-1*, *GhPIPLC4A-2*, *GhPIPLC4D-2*, *GhPIPLC4A-3*, and *GhPIPLC4D-3* may have an important role in salt stress response in cotton development, and the salt stress may be the driving force in the expansion of these six genes during the evolutionary process. To verify the role of these six GhPIPLCs in salt stress response, further investigations in the future, such as genetic verification experiments, are needed.

PI-specific phospholipase C is the key enzyme that catalyzes PIP_2 to produce IP_3 and DAG (Kadamur and Ross, 2013). IP_3, the critical secondary messenger that mediates calcium release from the ER, serves as the precursor in inositol phosphate biosynthesis and can be phosphorylated to form IP_6. Thus, IP_3 affects the downstream regulatory pathway of phytic acid (Xia and Yang, 2005). In this study, we discovered that IP_3 content in WT fibers was higher than that in WT and *fl* ovules at 10 DPA (Figure 2). Silencing *GhPIPLC2D* gene expression reduced IP_3 content and fiber length (Figure 3). These results suggest that IP_3 may contribute to cotton fiber elongation, which could be confirmed by observing the phenotypes resulting from stably transformed cotton plants. In addition, the *GhPIPLC2D* and *GhPIPLC2A* are allele and had similar expression patterns (Figure S2), suggesting both two genes might have similar functions. Silencing both *GhPIPLC2D* and *GhPIPLC2A* genes might have fiber length shorter than silencing only *GhPIPLC2D*, which needs to be further investigated.

A previous study revealed that linolenic acid promotes fiber elongation by activating PI and PIP biosynthesis (Liu et al., 2015). In eukaryotic cells, PI is the major phospholipid involved in a wide range of signaling pathways, such as hormone regulation, biotic and abiotic stress responses, and light response. PI is mainly phosphorylated to PIP_2, and then PIP_2 is cleaved to form IP_3 and DAG, which are two important secondary messengers in cells (Abd-El-Haliem and Joosten, 2017). Our data showed that exogenous application of C18:3 and PI significantly increased IP_3 and IP_6 contents, while *in vitro* applications of their inhibitors expectedly reduced IP_3 and IP_6 accumulation (Figure 5). Exogenous application of IP_6 significantly promoted cotton fiber length and the expression of ethylene biosynthesis genes (Figure 6). These results further indicate that IP_3 and IP_6 might play a critical role in cotton fiber elongation. The IP_6 contant measurement also showed that the IP_6 content was increased during fiber development (Figure S5). Meanwhile, exogenous applications of ethylene and IP_6 significantly improve the fiber length in *GhPIPLC2D*-silenced plant (Figure 7). Our study revealed that the *GhPIPLC2D* gene acts as a positive regulator in cotton fiber elongation, which the enzyme it encodes catalyzes PIP_2 to DAG and IP_3. Furthermore, IP_3 is phosphorylated to form IP_6 to promote cotton fiber elongation (Figure 8). In addition, previous study showed that phytic acid is mainly accumulated in the embryo of seed in maize, and it mainly provide phosphate and minerals for use during seedling growth and germination (Shi et al., 2003). The phosphorus was translocated to seed from roots and leaves and for synthesizing phytic acid and stored in seeds and it breakdown during germination for early seedling growth (Taliman et al., 2019). The 10 DPA ovules have the highest IP_6 content (Figure S5), indicating that IP_6 may also play important roles in ovule development.

Ethylene is a major phytohormone that participates in many developmental stages, such as cell division and root hair development (Song et al., 2019). In cotton, ethylene plays a major role in fiber cell elongation (Shi et al., 2003, 2006). One study showed that very-long-chain fatty acids promote fiber elongation by enhancing ethylene biosynthesis (Qin et al., 2007). In this study, we found that the expression of *GhACO1* and *GhACO3*, as well as ethylene production, were significantly decreased in *GhPIPLC2D*-silenced cotton compared with those of WT cotton (Figure 4). In addition, exogenous application of linolenic acid (C18:3), PI and IP_6 promoted ethylene biosynthesis (Figure 5). These results indicate that *GhPIPLC2D* and IP_3 promoted cotton fiber cell development possibly by activating ethylene biosynthesis and enhancing ethylene accumulation (Figure 8). This study provides empirical evidence that IP_3 regulates ethylene biosynthesis and promotes cotton fiber development, which is a branch in ethylene regulation of cotton fiber growth.

Calcium signals have been found to contribute to cotton fiber development (Guo et al., 2017). In *Arabidopsis*, *PIPLC* has been shown to be important in Ca^{2+} signaling, and *piplc3* mutants showed decreased Ca^{2+}

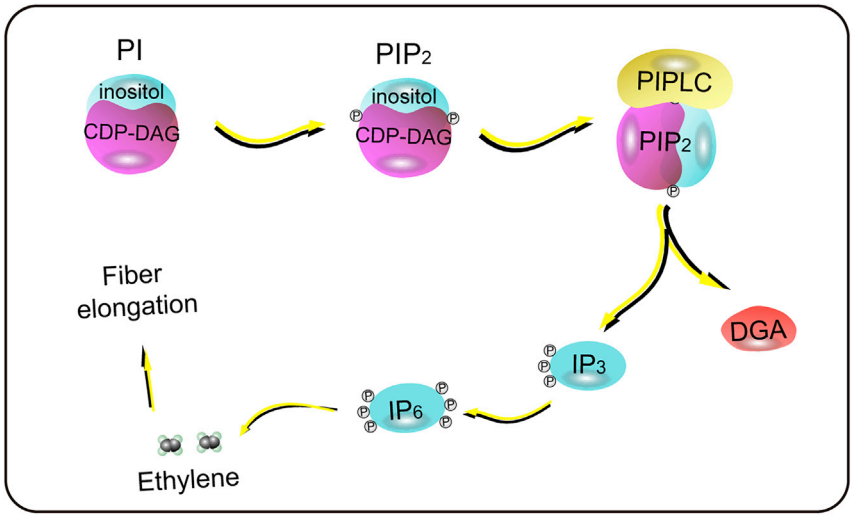

Figure 8. Proposed working model of *GhPIPLC* regulation of fiber elongation

release (Gao et al., 2014). The reductions of IP_3 and IP_6 levels affect Ca^{2+} release from the cytosol and might contribute to flg22-dependent cytosolic Ca^{2+} bursts (Hilleary et al., 2020). Moreover, Hasenstein and Evans (1986) found that Ca^{2+} enhances the conversion of 1-aminocyclopropane carboxylic acid (ACC) to ethylene in primary roots of corn. Yu et al. (2019) showed that Ca^{2+} promotes root development in response to salt stress by regulating the biosynthesis of ethylene. As a secondary messenger, Ca^{2+} is central for plant signal transduction. Calcium is involved in most environmental responses and phytohormone signal pathways (Peiter, 2011; Guo et al., 2017). Therefore, we speculate that *GhPIPLC2D* may also affect Ca^{2+} release and thus participate in fiber development in cotton. In the future, molecular mechanisms and regulatory relationships between *GhPIPLC2D*-Ca^{2+}-ethylene in regulating fiber cell elongation should be examined to deepen our understanding of the underlying processes in cotton fiber development.

Limitations of the study

In this study, we revealed a *GhPIPLC2D* gene serves as a positive regulator in cotton fiber elongation, which catalyzes PIP_2 to produce IP_3 and IP_3 promotes fiber elongation by enhancing ethylene biosynthesis. However, as we have discussed in the article, the *GhPIPLC2D* expression impact IP_3 content and IP_3 accumulation promote fiber elongation through enhancing ethylene biosynthesis while the *GhPIPLC2D*-ethylene in regulating fiber cell elongation should be examined to deepen our understanding of the underlying processes in cotton fiber development. In addition, how IP_3 promotes ethylene synthesis also needs to be further clarified in future studies.

Resource availability

Lead contact

Further information and requests for resources should be directed to and will be fulfilled by the lead contact, Guanghui Xiao (guanghuix@snnu.edu.cn).

Materials availability

This study did not generate new unique reagents.

Data and code availability

This study did not generate or analyze data sets and code.

METHODS

All methods can be found in the accompanying Transparent methods supplemental file.

SUPPLEMENTAL INFORMATION

Supplemental information can be found online at https://doi.org/10.1016/j.isci.2021.102199.

ACKNOWLEDGMENTS

This work is supported by the National Natural Science Foundation of China (32070549), Natural Science Basic Research Plan in the Shaanxi Province of China (2019JQ-062 and 2020JQ-410), Shaanxi Youth Entrusted Talent Program (20190205), Shaanxi Postdoctoral Project (2018BSHYDZZ76), Fundamental Research Funds for the Central Universities (GK201903064, GK202002005 and GK202001004), Young Elite Scientists Sponsorship Program by CAST (2019-2021QNRC001) and State Key Laboratory of Cotton Biology Open Fund (CB2020A12).

AUTHOR CONTRIBUTIONS

L.Z. and D.L. performed the experiments; L.Z. and H.S. analyzed the data; L.Z., D.L., and H.S. performed software application and data visualization; L.Z. and G.X. wrote the paper; G.X., J.Y., and H.L. conceived and designed the experiments. All authors read and approved the final manuscript.

DECLARATION OF INTERESTS

The authors declare that they have no conflict of interests.

Received: August 8, 2020
Revised: January 13, 2021
Accepted: February 12, 2021
Published: March 19, 2021

REFERENCES

Abd-El-Haliem, A.M., and Joosten, M.H. (2017). Plant phosphatidylinositol-specific phospholipase C at the center of plant innate immunity. J. Integr. Plant Biol. *59*, 164–179.

Alimohammadi, M., de Silva, K., Ballu, C., Ali, N., and Khodakovskaya, M.V. (2012). Reduction of inositol (1,4,5)-trisphosphate affects the overall phosphoinositol pathway and leads to modifications in light signalling and secondary metabolism in tomato plants. J. Exp. Bot. *63*, 825–835.

Arpat, A.B., Waugh, M., Sullivan, J.P., Gonzales, M., Frisch, D., Main, D., Wood, T., Leslie, A., Wing, R.A., and Wilkins, T.A. (2004). Functional genomics of cell elongation in developing cotton fibers. Plant Mol. Biol. *54*, 911–929.

Blatt, M.R., Thiel, G., and Trentham, D.R. (1990). Reversible inactivation of K^+ channels of Vicia stomatal guard cells following the photolysis of caged inositol 1,4,5-trisphosphate. Nature *346*, 766–769.

Chu, Y.J., Chen, X., and Xue, H.W. (2016). Ins(1,4,5)P3 suppresses protein degradation in plant vacuoles by regulating SNX-mediated protein sorting. Mol. Plant *9*, 1440–1443.

Conte, G., Dimauro, C., Serra, A., Macciotta, N.P.P., and Mele, M. (2018). A canonical discriminant analysis to study the association between milk fatty acids of ruminal origin and milk fat depression in dairy cows. J. Dairy Sci. *101*, 6497–6510.

D'Ambrosio, J.M., Couto, D., Fabro, G., Scuffi, D., Lamattina, L., Munnik, T., Andersson, M.X., Alvarez, M.E., Zipfel, C., and Laxalt, A.M. (2017). Phospholipase C2 affects MAMP-triggered immunity by modulating ROS production. Plant Physiol. *175*, 970–981.

Di Fino, L.M., D'Ambrosio, J.M., Tejos, R., van Wijk, R., Lamattina, L., Munnik, T., Pagnussat, G.C., and Laxalt, A.M. (2017). Arabidopsis phosphatidylinositol-phospholipase C2 (PLC2) is required for female gametogenesis and embryo development. Planta *245*, 717–728.

Dong, J., Ma, G., Sui, L., Wei, M., Satheesh, V., Zhang, R., Ge, S., Li, J., Zhang, T.E., Wittwer, C., et al. (2019). Inositol pyrophosphate InsP8 acts as an intracellular phosphate signal in *Arabidopsis*. Mol. Plant *12*, 1463–1473.

Drayer, A., Meima, M., Derks, M.W., Tuik, R., and van Haastert, P. (1995). Mutation of an EF-hand Ca(2+)-binding motif in phospholipase C of dictyostelium discoideum: inhibition of activity but no effect on Ca(2+)-dependence. Biochem. J. *311*, 505–510.

Gao, K., Liu, Y.L., Li, B., Zhou, R.G., Sun, D.Y., and Zheng, S.Z. (2014). Arabidopsis thaliana phosphoinositide-specific phospholipase C isoform 3 (AtPLC3) and AtPLC9 have an additive effect on thermotolerance. Plant Cell Physiol. *55*, 1873–1883.

Gibson, R., Raboy, V., and King, J. (2018). Implications of phytate in plant-based foods for iron and zinc bioavailability, setting dietary requirements, and formulating programs and policies. Nutr. Rev. *76*, 793–804.

Guo, K., Tu, L., He, Y., Deng, J., Wang, M., Huang, H., Li, Z., and Zhang, X. (2017). Interaction between calcium and potassium modulates elongation rate in cotton fiber cells. J. Exp. Bot. *68*, 5161–5175.

Hänninen, S., Batchu, K., Hokynar, K., and Somerharju, P. (2017). Simple and rapid biochemical method to synthesize labeled or unlabeled phosphatidylinositol species. J. Lipid Res. *58*, 1259–1264.

Hasenstein, K., and Evans, M. (1986). Calcium ion dependency of ethylene production in segments of primary roots of Zea mays. Physiol. Plant *67*, 570–575.

He, P., Yang, Y., Wang, Z., Zhao, P., Yuan, Y., Zhang, L., Ma, Y., Pang, C., Yu, J., and Xiao, G. (2019). Comprehensive analyses of ZFP gene family and characterization of expression profiles during plant hormone response in cotton. BMC Plant Biol. *19*, 329.

Heilmann, I. (2016). Phosphoinositide signaling in plant development. Development *143*, 2044–2055.

Hempel, F., Stenzel, I., Heilmann, M., Krishnamoorthy, P., Menzel, W., Golbik, R., Helm, S., Dobritzsch, D., Baginsky, S., Lee, J., et al. (2017). MAPKs influence pollen tube growth by controlling the formation of phosphatidylinositol 4,5-bisphosphate in an apical plasma membrane domain. Plant Cell *29*, 3030–3050.

Hilleary, R., Paez-Valencia, J., Vens, C., Toyota, M., Palmgren, M., and Gilroy, S. (2020). Tonoplast-localized Ca2+ pumps regulate Ca2+ signals during pattern-triggered immunity in Arabidopsis thaliana. Proc. Natl. Acad. Sci. U S A *117*, 18849–18857.

Hu, H., Wang, M., Ding, Y., Zhu, S., Zhao, G., Tu, L., and Zhang, X. (2018). Transcriptomic repertoires depict the initiation of lint and fuzz fibres in cotton (*Gossypium hirsutum* L.). Plant Biotechnol. J. *16*, 1002–1012.

Hui, Q., Wang, M., Wang, P., Ma, Y., Gu, Z., and Yang, R. (2018). Gibberellic acid promoting phytic acid degradation in germinating soybean under calcium lactate treatment. J. Sci. Food Agric. *98*, 644–651.

Jiao, C., Chai, Y., and Duan, Y. (2019). Inositol 1,4,5-trisphosphate mediates nitric-oxide-induced chilling tolerance and defense response in postharvest peach fruit. J. Agric. Food Chem. *67*, 4764–4773.

Kadamur, G., and Ross, E.M. (2013). Mammalian phospholipase C. Annu. Rev. Physiol. *75*, 127–154.

Kato, M., Tsuge, T., Maeshima, M., and Aoyama, T. (2019). *Arabidopsis* PCaP2 modulates the phosphatidylinositol 4,5-bisphosphate signal on the plasma membrane and attenuates root hair elongation. Plant J. *99*, 610–625.

Kim, H.J., and Triplett, B.A. (2001). Cotton fiber growth in planta and in vitro. Models for plant cell elongation and cell wall biogenesis. Plant Physiol. *127*, 1361–1366.

Kusano, H., Testerink, C., Vermeer, J.E., Tsuge, T., Shimada, H., Oka, A., Munnik, T., and Aoyama, T. (2008). The Arabidopsis phosphatidylinositol phosphate 5-Kinase PIP5K3 is a key regulator of root hair tip growth. Plant Cell *20*, 367–380.

Lee, H.S., Lee, D.H., Cho, H.K., Kim, S.H., Auh, J.H., and Pai, H.S. (2015). InsP6-sensitive variants of the Gle1 mRNA export factor rescue growth and fertility defects of the ipk1 low-phytic-acid mutation in *Arabidopsis*. Plant Cell *27*, 417–431.

Lemtiri-Chlieh, F., MacRobbie, E.A., Webb, A.A., Manison, N.F., Brownlee, C., Skepper, J.N., Chen, J., Prestwich, G.D., and Brearley, C.A. (2003). Inositol hexakisphosphate mobilizes an endomembrane store of calcium in guard cells. Proc. Natl. Acad. Sci. U S A *100*, 10091–10095.

Li, F., Fan, G., Lu, C., Xiao, G., Zou, C., Kohel, R.J., Ma, Z., Shang, H., Ma, X., Wu, J., et al. (2015). Genome sequence of cultivated Upland cotton (*Gossypium hirsutum* TM-1) provides insights into genome evolution. Nat. Biotechnol. *33*, 524–530.

Li, H.B., Qin, Y.M., Pang, Y., Song, W.Q., Mei, W.Q., and Zhu, Y.X. (2007). A cotton ascorbate peroxidase is involved in hydrogen peroxide homeostasis during fibre cell development. New Phytol. *175*, 462–471.

Li, L., Wang, F., Yan, P., Jing, W., Zhang, C., Kudia, J., and Zhang, W. (2017). A phosphoinositide-specific phospholipase C pathway elicits stress-induced Ca2+ signals and confers salt tolerance to rice. New Phytol *214*, 1172–1187.

Liu, G.J., Xiao, G.H., Liu, N.J., Liu, D., Chen, P.S., Qin, Y.M., and Zhu, Y.X. (2015). Targeted lipidomics studies reveal that linolenic acid promotes cotton fiber elongation by activating phosphatidylinositol and phosphatidylinositol monophosphate biosynthesis. Mol. Plant *8*, 911–921.

Lv, F., Wang, H., Wang, X., Han, L., Ma, Y., Wang, S., Feng, Z., Niu, X., Cai, C., Kong, Z., et al. (2015). GhCFE1A, a dynamic linker between the ER network and actin cytoskeleton, plays an important role in cotton fibre cell initiation and elongation. J. Exp. Bot. *66*, 1877–1889.

Menzel, W., Stenzel, I., Helbig, L.M., Krishnamoorthy, P., Neumann, S., Eschen-Lippold, L., Heilmann, M., Lee, J., and Heilmann, I. (2019). A PAMP-triggered MAPK cascade inhibits phosphatidylinositol 4,5-bisphosphate production by PIP5K6 in *Arabidopsis thaliana*. New Phytol. *224*, 833–847.

Mueller-Roeber, B., and Pical, C. (2002). Inositol phospholipid metabolism in *Arabidopsis*. Characterized and putative isoforms of inositol phospholipid kinase and phosphoinositide-specific phospholipase C. Plant Physiol. *130*, 22–46.

Munnik, T., and Nielsen, E. (2011). Green light for polyphosphoinositide signals in plants. Curr. Opin. Plant Biol. *14*, 489–497.

Peiter, E. (2011). The plant vacuole: emitter and receiver of calcium signals. Cell Calcium *50*, 120–128.

Pokotylo, I., Kolesnikov, Y., Kravets, V., Zachowski, A., and Ruelland, E. (2014). Plant phosphoinositide-dependent phospholipases C: variations around a canonical theme. Biochimie *96*, 144–157.

Qin, Y.M., Hu, C.Y., Pang, Y., Kastaniotis, A.J., Hiltunen, J.K., and Zhu, Y.X. (2007). Saturated very-long-chain fatty acids promote cotton fiber and *Arabidopsis* cell elongation by activating ethylene biosynthesis. Plant Cell *19*, 3692–3704.

Sharif, I., Aleem, S., Farooq, J., Rizwan, M., Younas, A., Sarwar, G., and Chohan, S.M. (2019). Salinity stress in cotton: effects, mechanism of tolerance and its management strategies. Physiol. Mol. Biol. Plants *25*, 807–820.

Shi, J., Wang, H., Wu, Y., Hazebroek, J., Meeley, R.B., and Ertl, D.S. (2003). The maize low-phytic acid mutant lpa2 is caused by mutation in an inositol phosphate kinase gene. Plant Physiol. *131*, 507–515.

Shi, Y.H., Zhu, S.W., Mao, X.Z., Feng, J.X., Qin, Y.M., Zhang, L., Cheng, J., Wei, L.P., Wang, Z.Y., and Zhu, Y.X. (2006). Transcriptome profiling, molecular biological, and physiological studies reveal a major role for ethylene in cotton fiber cell elongation. Plant Cell *18*, 651–664.

Shimada, T.L., Betsuyaku, S., Inada, N., Ebine, K., Fujimoto, M., Uemura, T., Takano, Y., Fukuda, H., Nakano, A., and Ueda, T. (2019). Enrichment of phosphatidylinositol 4,5-bisphosphate in the extra-invasive hyphal membrane promotes colletotrichum infection of Arabidopsis thaliana. Plant Cell Physiol. *60*, 1514–1524.

Singh, A., Bhatnagar, N., Pandey, A., and Pandey, G.K. (2015). Plant phospholipase C family: regulation and functional role in lipid signaling. Cell Calcium *58*, 139–146.

Singh, A., Kanwar, P., Pandey, A., Tyagi, A.K., Sopory, S.K., Kapoor, S., and Pandey, G.K. (2013). Comprehensive genomic analysis and expression profiling of phospholipase C gene family during abiotic stresses and development in rice. PLoS One *8*, e62494.

Song, W., Wang, F., Chen, L., Ma, R., Zuo, X., Cao, A., Xie, S., Chen, X., Jin, X., and Li, H. (2019). GhVTC1, the key gene for ascorbate biosynthesis in *Gossypium hirsutum*, involves in cell elongation under control of ethylene. Cells *8*, 1039.

Taliman, N.A., Dong, Q., Echigo, K., Raboy, V., and Saneoka, H. (2019). Effect of phosphorus fertilization on the growth, photosynthesis, nitrogen fixation, mineral accumulation, seed yield, and seed quality of a soybean low-phytate line. Plants *8*, 119.

Tan, X., Calderon-Villalobos, L.I., Sharon, M., Zheng, C., Robinson, C.V., Estelle, M., and Zheng, N. (2007). Mechanism of auxin perception by the TIR1 ubiquitin ligase. Nature *446*, 640–645.

Tasma, I.M., Brendel, V., Whitham, S.A., and Bhattacharyya, M.K. (2008). Expression and evolution of the phosphoinositide-specific phospholipase C gene family in Arabidopsis thaliana. Plant Physiol. Biochem. *46*, 627–637.

Van Wijk, R., Zhang, Q., Zarza, X., Lamers, M., Marquez, F.R., Guardia, A., Scuffi, D., Garcia-Mata, C., Ligterink, W., Haring, M.A., et al. (2018). Role for *Arabidopsis* plc7 in stomatal movement, seed mucilage attachment, and leaf serration. Front. Plant Sci. *9*, 1721.

Wu, H., Tian, Y., Wan, Q., Fang, L., Guan, X., Chen, J., Hu, Y., Ye, W., Zhang, H., Guo, W., et al. (2017). Genetics and evolution of MIXTA genes regulating cotton lint fiber development. New Phytol. *217*, 883–895.

Xia, H.J., and Yang, G. (2005). Inositol 1,4,5-trisphosphate 3-kinases: functions and regulations. Cell Res. *15*, 83–91.

Xiao, G., Zhao, P., and Zhang, Y. (2019). A pivotal role of hormones in regulating cotton fiber development. Front. Plant Sci. *10*, 87.

Xiao, G., Wang, K., Huang, G., and Zhu, Y. (2016). Genome-scale analysis of the cotton KCS gene family revealed a binary mode of action for gibberellin A regulated fiber growth. J. Integr. Plant Biol. *58*, 577–589.

Yu, J., Niu, L., Yu, J., Liao, W., Xie, J., Lv, J., Feng, Z., Hu, L., and Dawuda, M. (2019). The involvement of ethylene in calcium-induced adventitious root formation in cucumber under salt stress. Int. J. Mol. Sci. *20*, 1047.

Zhang, B., Wang, Y., and Liu, J.Y. (2018a). Genome-wide identification and characterization of phospholipase C gene family in cotton (Gossypium spp.). Sci. China Life Sci. *61*, 88–99.

Zhang, J., Huang, G., Zou, D., Yan, J., Li, Y., Hu, S., and Li, X. (2018b). The cotton (*Gossypium hirsutum*) NAC transcription factor (FSN1) as a positive regulator participates in controlling secondary cell wall biosynthesis and modification of fibers. New Phytol. *217*, 625–640.

Zhang, M., Zheng, X., Song, S., Zeng, Q., Hou, L., Li, D., Zhao, J., Wei, Y., Li, X., Luo, M., et al. (2011). Spatiotemporal manipulation of auxin biosynthesis in cotton ovule epidermal cells enhances fiber yield and quality. Nat. Biotechnol. *29*, 453–458.

Zhang, Q., Van Wijk, R., Zarza, X., Shahbaz, M., van Hooren, M., Guardia, A., Scuffi, D., Garcia-Mata, C., Van den Ende, W., Hoffmann-Benning, S., et al. (2018c). Knock-down of Arabidopsis plc5 reduces primary root growth and secondary root formation while overexpression improves drought tolerance and causes stunted root hair growth. Plant Cell Physiol. *59*, 2004–2019.

Zheng, S.Z., Liu, Y.L., Li, B., Shang, Z.L., Zhou, R.G., and Sun, D.Y. (2012). Phosphoinositide-specific phospholipase C9 is involved in the thermotolerance of Arabidopsis. Plant J. *69*, 689–700.

iScience, Volume *24*

Supplemental information

GhPIPLC2D promotes cotton fiber elongation by enhancing ethylene biosynthesis

Liping Zhu, Lingling Dou, Haihong Shang, Hongbin Li, Jianing Yu, and Guanghui Xiao

Supplemental Information

Transparent Methods

Phylogenetic and domain analysis of GhPIPLCs

Multiple amino acid sequences of PIPLCs from *A. thaliana* (Tasma et al., 2008), *O. sativa* (Singh et al., 2013), *G. arboreum* (Du et al., 2018), *G. herbaceum* (Huang et al., 2020), *G. raimondii* (Wang et al., 2012) and *G. hirsutum* (Zhang et al., 2018a) were obtained to construct a phylogenetic tree using MEGA 7.0 software (Kumar et al., 2016) and the neighbor-joining statistical method with 1000 bootstrap replications. The GhPIPLCs were renamed according to the phylogenetic relationships of GhPIPLCs and AtPIPLCs; the names and corresponding genome ID information of GhPIPLCs are shown in Supplementary Table 1. The amino acid sequences of all GhPIPLCs were then submitted to an online bioinformatic tool Pfam (http://pfam.xfam.org/) to investigate the conserved domain information.

Plant materials and *in vitro* ovule culture

The cultivar of upland cotton Xuzhou-142 wild-type (WT) and its *fuzzless-lintless* mutant (*fl*) produced from WT plants as well as *GhPIPLC2D*-silenced plants were grown in a greenhouse at 60% humidity, 25 °C, and a 16-h/8-h light/dark cycle. Cotton bolls were picked at -3, 0, +3, +5, +10, +15 and +20 days post-anthesis from both WT and mutant plants. The fibers and ovules at -3 to +20 DPA were stored in liquid nitrogen until use. The XJ128 Rapid Fiber Tester (ChangLing, China) was used for fiber length detection following the standard test methods of the manufacturer. Ovules were obtained at anthesis and then sterilized using 10% sodium hypochlorite solution prior to culturing. For the C18 fatty acid, PI, IP_6 and ethylene treatment assays, 5 μM of each C18:0, C18:1, C18:2, C18:3, and PI; 0.5–1 μM of the C18:3 inhibitor carbenoxolone; 0.5–1 μM of the PI inhibitor 5-hydroxytryptamine; or 1–10 μM of IP_6 and 2 μM of ethephon were cultured with cotton ovules in the culture medium formulated by Beasley and Ting (1973) at 30 °C under aseptic conditions (Shi et al., 2006). The composition of the culture medium was as follows: 272.18 mg/L KH_2PO_4, 6.183 mg/L H_3BO_3, 0.242 mg/L $Na_2MoO_4{\cdot}2H_2O$, 441.06 mg/L $CaCl_2{\cdot}2H_2O$, 0.83 mg/L KI, 0.024 mg/L $CoCl_2{\cdot}6H_2O$, 493 mg/L $MgSO_4{\cdot}7H_2O$, 16.902 mg/L $MnSO_4{\cdot}H_2O$, 8.627 mg/L $ZnSO_4{\cdot}7H_2O$, 0.025 mg/L $CuSO_4{\cdot}5H_2O$, 5055.5 mg/L KNO_3, 8.341 mg/L $FeSO_4{\cdot}7H_2O$, 11.167 mg/L Na_2EDTA, 0.492 mg/L nicotinic acid (vitamin B3), 0.822 mg/L pyridoxine·HCL (vitamin B6), 1.349 mg/L thiamine·HCL (vitamin B1), 180.16 mg/L myo-inositol, 18016 mg/L D-glucose and 3603.2 mg/L D-fructose. The pH was 6.0.

RNA extraction and quantitative real-time PCR

Total RNA from fibers and ovules were extracted using the Invitrogen RNeasy kit (Life Technologies, USA). First-strand complementary DNA (cDNA) were reverse-transcribed from 2 μg total RNA using the standard procedure described in the kit's manual, including the DNase treatment steps (Takara, Japan). The qRT-PCR was performed using gene-specific primers listed in Supplementary Table 3. We used *UBQ7* (GenBank No. AY189972) as the internal control. The reactions, with samples having three technical replicates, were performed using the Roche Light Cycle 480 II instrument (Roche, Basel, Switzerland). One reaction contained 0.5 μL cDNA (10 ng), 10 μL SYBR/ROX qPCR Mix (2×), 0.75 μL forward primer, 0.75 μL reverse primer and 8 μL ddH_2O. The qPCR reaction was performed as follows: 95°C for 3 min followed by 40 cycles of 95°C for 25 s, 56°C for 30 s and 72°C for 30 s. Fluorescence signals were automatically acquired at the end of each cycle. The $2^{-\Delta\Delta CT}$ method was used to calculate the relative expression levels of the target genes. Three independent biological replications were carried out for each gene. The Multi Experiment Viewer (MeV, version 4.9, Boston, MA, USA) software was used to generate gene expression heat maps.

Virus-induced gene silencing (VIGS) and cotton plant transformation

We used *Cotton leaf crumple virus* (CLCrV)-based vectors (i.e., pCLCrV-A and pCLCrV-B) for the VIGS experiment (Gu et al., 2014). The 429-bp *GhPIPLC2D* gene fragment was amplified from total cDNAs with primers listed in Supplementary Table S3. A total of nine plants were used for the VIGS experiment, consisting of three biological replicates. The PCR products were digested with *Spe*I and *Asc*I (detailed information of the restriction sites are attached in Supplementary Table 3) and then ligated into the pCLCrV-A vector using NEB T4 DNA ligase (New England BioLabs, Ipswich, MA). We followed the manufacturer's protocol supplied with the ligase. The constructs (pCLCrV: *GhPIPLC2D*, pCLCrV-A, and pCLCrV-B) were individually introduced into *Agrobacterium tumefaciens* strain LBA4404. The *Agrobacterium* colonies containing pCLCrV:*GhPIPLC2D*, pCLCrV-A, or pCLCrV-B were grown for 24 h at 28 °C. Then the *Agrobacterium* cells were collected and resuspended in infiltration medium (10 mM $MgCl_2$, 10 mM MES, and 200 mM acetosyringone) and cultured to OD600 = 1.2. The *Agrobacterium* cells containing pCLCrV-B were mixed with either the culture of *Agrobacterium* cells with pCLCrV:*GhPIPLC2D* or pCLCrV-A at a ratio of 1:1. Each mixture was injected into three cotton seedling cotyledons (about 10-day-old seedlings) for the silencing experiment. After a 24-h incubation in darkness, the seedlings were grown at 25°C under a 16-h light, 8-h dark cycle.

IP_3 content determination

Extraction of IP_3 was performed using a method described previously (Burnette et al., 2003). The IP_3 content was determined by using the Inositol-1,4,5-Trisphosphate [^{3}H] Radioreceptor Assay Kit (PerkinElmer Life Sciences, Finland) and a standard curve derived from known concentrations of IP_3.

Cotton fatty acid extraction and Gas chromatography–mass spectrometry

Fatty acids were extracted from 20 mg flower, leaf, root and stem tissues from four-month-old cotton plants and from the ovules at 10 days post-anthesis. Subsequently, they were freeze-dried and then immersed in chloroform/methanol (2:1, v/v) for 1 min to remove surface waxes (Qin et al., 2007). Cotton samples were homogenized in liquid nitrogen and extracted with 2.5% H_2SO_4 in methanol (v/v). Heptadecanoic acid (C17:0), as the internal standard, was added into the fatty acid extraction medium to monitor fatty acid recovery and quantification. Then the fatty acid methyl esters were dissolved in hexane. A 1 μL sample was injected into the Agilent 6890N GC system (Agilent, California, USA). Fatty acids were measured by an HP 5975 mass selective detector (HP, California, USA) connected to the GC system using the method described previously (Liu et al., 2015).

Ethylene content measurements

Twenty 1 DPA ovules were freshly-collected and then cultured in a 96-well culture plate with 150 μL liquid media containing 5 μM linolenic acid, 2 μM PI, 1 μM carbenoxolone or 1 μM 5-hydroxytryptamine for 6 d at 30°C. Air samples (100 μL) from each well were collected with a sample injector and injected into the gas chromatograph column held at 60°C for 20 min with nitrogen as the carrier gas. A gas chromatograph (GC6890N; Agilent) equipped with a flame-ionization detector and a HP-PLOT column (30 m × 530 μm × 40 μm, Agilent Technologies) was used to perform ethylene measurements. Standards of 0.1, 1, 10, and 50 ppm ethylene were used to determine the amount of ethylene production. All experiments were performed with three replicates. Statistical significance was determined using one-way ANOVA with Tukey's test in this research.

SUPPLEMENTAL REFERENCES

Ting, B. I. P. (1973). The effects of plant growth substances on *in vitro* fiber development from fertilized cotton ovules. Amer. J. Bot. 60,130–139.

Burnette, R.N., Gunesekera, B.M., and Gillaspy, G.E. (2003). An Arabidopsis inositol 5-phosphatase gain-of-function alters abscisic acid signaling. Plant Physiol. 132, 1011–1019.

Du, X., Huang, G., He, S., Sun, G, Ma, X., Li, N., Zhang, X., Sun, J., Liu, M., et al. (2018). Resequencing of 243 diploid cotton accessions based on an updated A genome identifies the genetic basis of key agronomic traits. Nat. Genet. 50, 796–802.

Gu, Z., Huang, C., Li, F., and Zhou, X. (2014). A versatile system for functional analysis of genes and microRNAs in cotton. Plant Biotechnol. J. 12, 638–649.

Huang, G., Wu, Z., Percy, R. G., Bai, M., Li, Y., Frelichowski, J. E., Hu, J., Wang, K., Yu, J. Z., & Zhu, Y. (2020). Genome sequence of *Gossypium herbaceum* and genome updates of *Gossypium arboreum* and *Gossypium hirsutum* provide insights into cotton A-genome evolution. Nat. Genet. 52, 516–524.

Kumar, S., Stecher, G., and Tamura, K. (2016). MEGA7: Molecular evolutionary genetics analysis version 7.0 for bigger datasets. Mol. Biol. Evol. 33, 1870–1874.

Wang, K., Wang, Z., Li, F., Ye, W., Wang, J., Song, G., Yue, Z., Cong, L., Shang, H., Zhu, S., et al. (2012). The draft genome of a diploid cotton *Gossypium raimondii*. Nat. Genet. 44, 1098–1103.

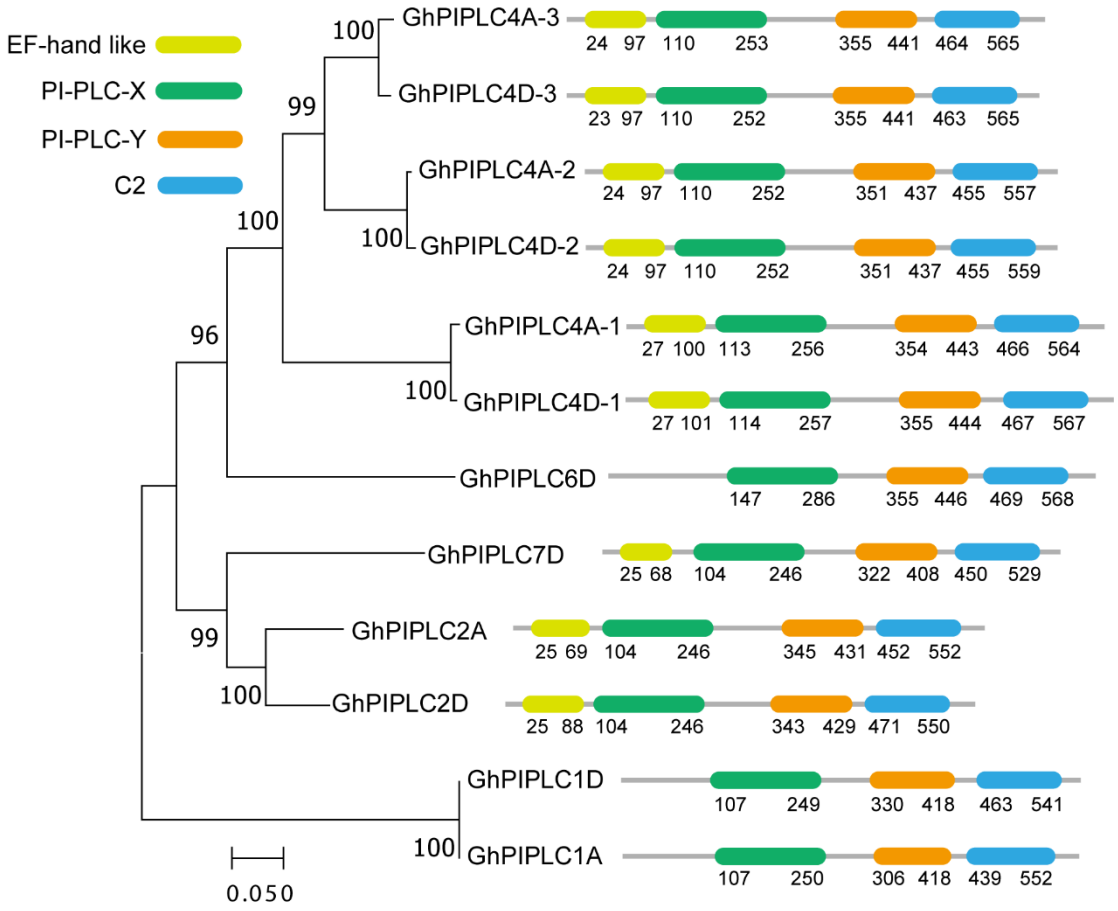

Figure S1. Phylogenetic and conserved domain analysis of GhPIPLCs, Related to Figure 1.

Gray lines indicate protein sequence lengths. Boxes with different colors represent different conserved domains. Numbers under the boxes show the specific location of each domain.

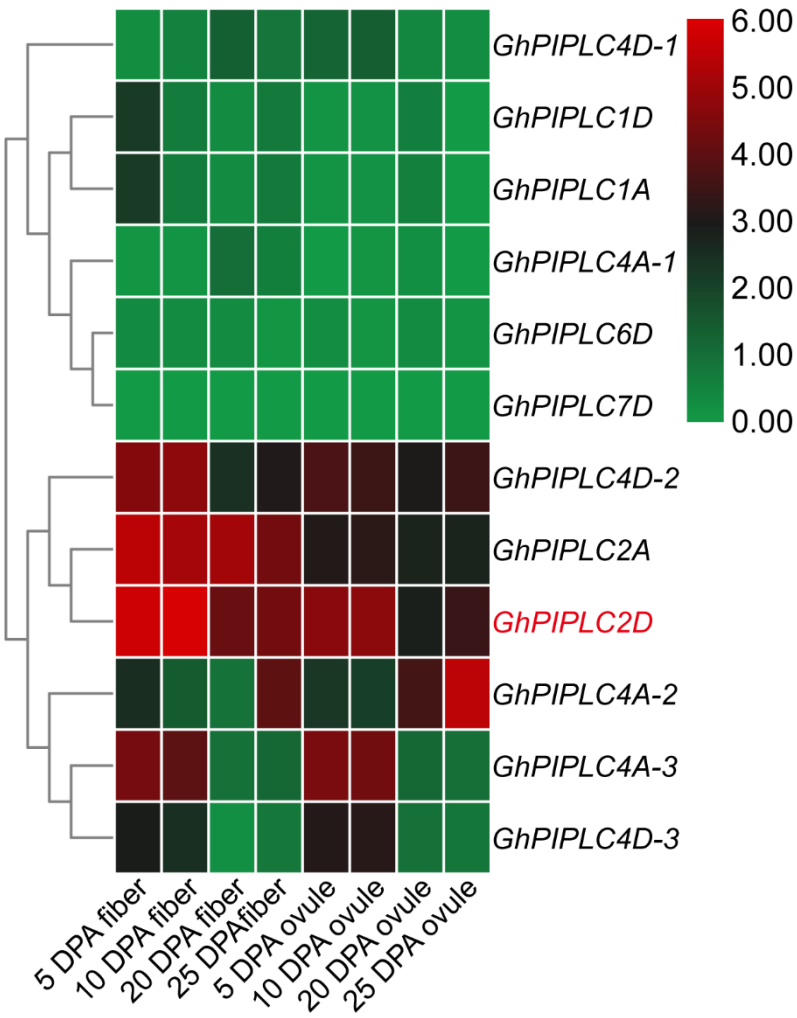

Figure S2. Expression profiles of *GhPIPLC* over time of fiber and ovule development, Related to Figure 2.

Expression patterns of genes were clustered. Green and red colors indicate low and high transcriptional expression levels, respectively. The *GhPIPLC2D* genes (in red font) were selected for further functional analysis. DPA, days post-anthesis.

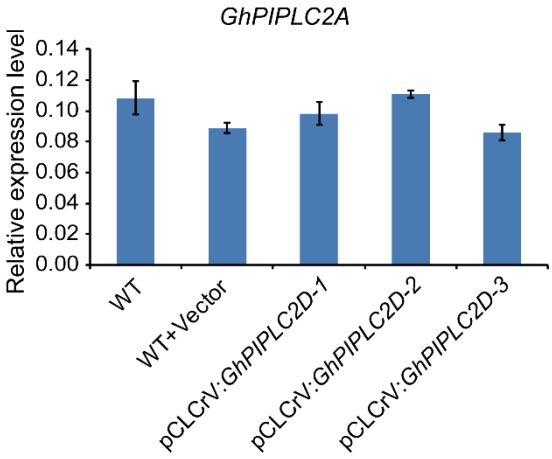

Figure S3. Relative expression levels of *GhPIPLC2A* in *GhPIPLC2D*-silenced cotton, Related to Figure 3.

Gene expression data were obtained by quantitative real-time PCR with three independent replicates. Statistical significance was determined using one-way ANOVA with Tukey's test. Error bars represent the SE (n = 3 biological replicates).

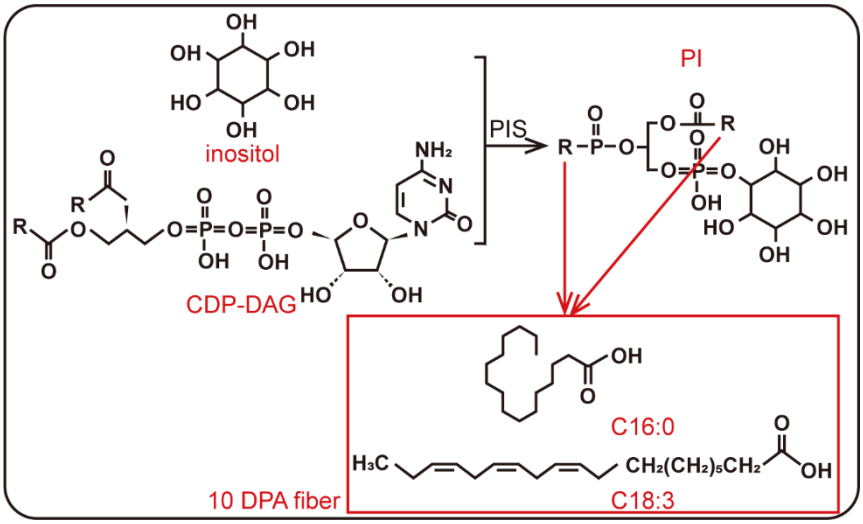

Figure S4. Structural formula of phosphatidylinositol (PI) biosynthesis, Related to Figure 5.

C16:0, palmitic acid. C18:3, linolenic acid. PIS, phosphatidylinositol synthase. CDP-DAG, CDP-diacylglycerol. DPA, days post-anthesis. The two fatty acids in the red box represent the most abundant fatty acids of PI in 10 DPA fiber.

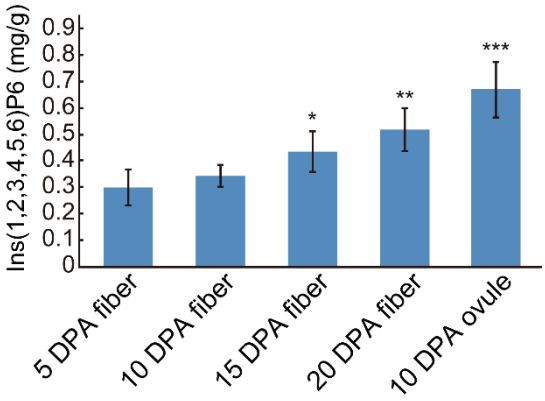

Figure S5. Accumulation of IP_6 in ovules and fibers at different developmental stages, Related to Figure 5.

Statistical significance was determined using one-way ANOVA with Tukey's test. Error bars represent the SE (n = 3 biological replicates). $^{**}P < 0.01$. No chemicals were added to the control.

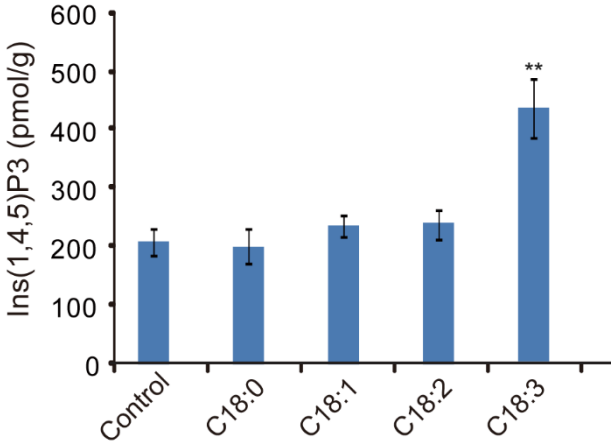

Figure S6. Accumulation of IP_3 after exogenous application of C18:0, C18:1, C18:2 or C18:3, Related to Figure 5.

Statistical significance was determined using one-way ANOVA with Tukey's test. Error bars represent the SE (n = 3 biological replicates). $^{**}P < 0.01$. No chemicals were added to the control.

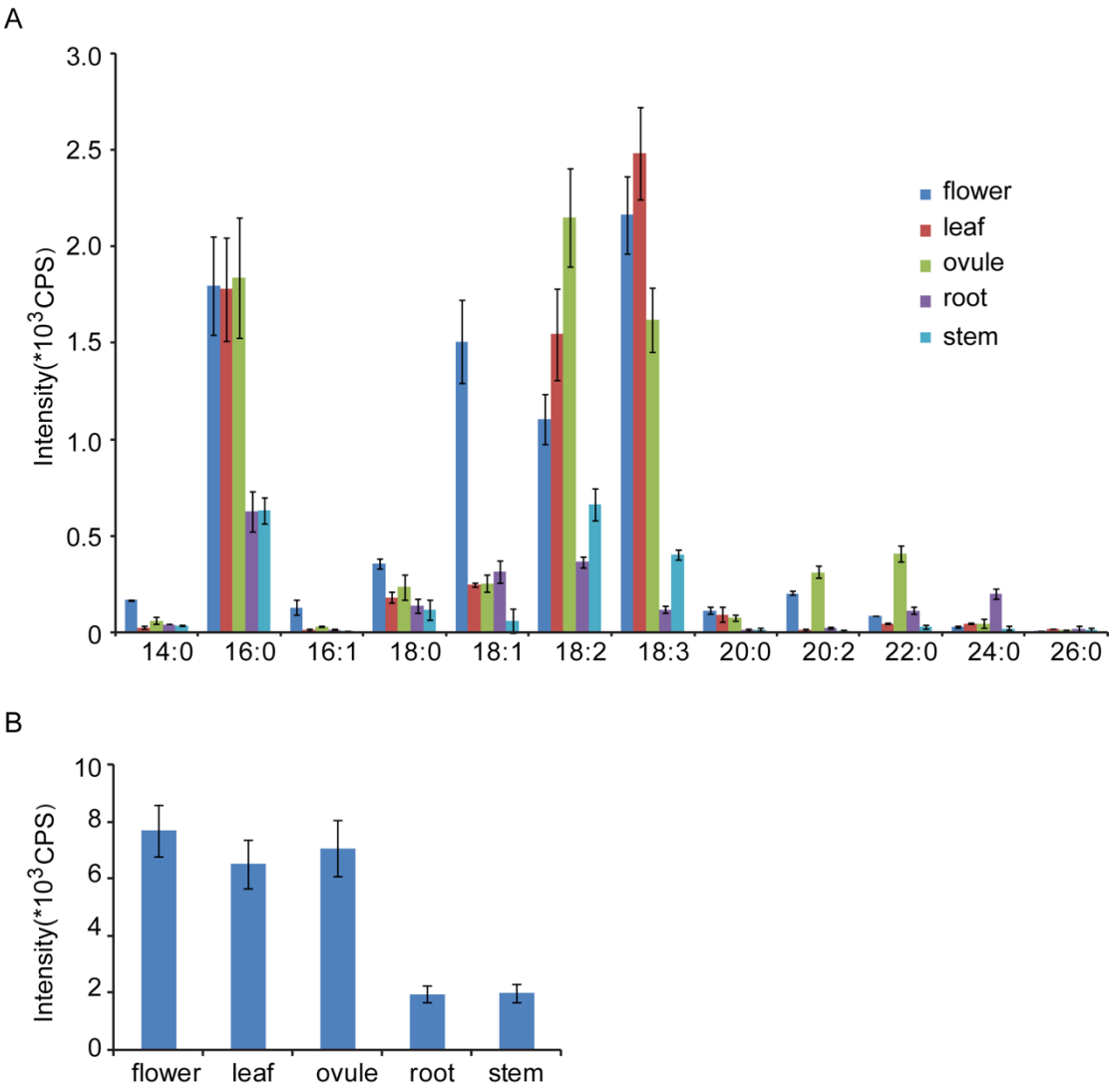

Figure S7. Fatty acid accumulation in five different cotton plant tissues, Related to Figure 5.

(A) intensities of different types of fatty acids.

(B) intensities of total fatty acids. Error bars represent the SE (n = 3 biological replicates).

Table S1. Given names (New Name) of *GhPIPLC*s used in this study corresponding to their names and genome IDs obtained from Zhang et al., (2018a), Related to Figure 1.

New Name	Name	ID
GhPIPLC1D	*GhPIPLC4*	CotAD_09433
GhPIPLC1A	*GhPIPLC9*	CotAD_18525
GhPIPLC2A	*GhPIPLC5*	CotAD_62184
GhPIPLC2D	*GhPIPLC11*	CotAD_22832
GhPIPLC4A-1	*GhPIPLC3*	CotAD_09434
GhPIPLC4D-1	*GhPIPLC8*	CotAD_18524
GhPIPLC4A-2	*GhPIPLC2*	CotAD_09425
GhPIPLC4D-2	*GhPIPLC7*	CotAD_18522
GhPIPLC4A-3	*GhPIPLC1*	CotAD_56315
GhPIPLC4D-3	*GhPIPLC6*	CotAD_30245
GhPIPLC6D	*GhPIPLC10*	CotAD_22531
GhPIPLC7D	*GhPIPLC12*	CotAD_22314

Table S2. Analysis of duplication events of *PIPLC4* genes from *G. hirsutum*, *G. arboreum*, *G. herbaceum* and *G. raimondii*, Related to Figure 1.

CotAD_56315	GhPIPLC4A-3	Whole Genome/Segmental Duplication
CotAD_30245	GhPIPLC4D-3	Whole Genome/Segmental Duplication
CotAD_09425	GhPIPLC4A-2	Tandem duplication
CotAD_09434	GhPIPLC4A-1	Tandem duplication
CotAD_18522	GhPIPLC4D-2	Tandem duplication
CotAD_18524	GhPIPLC4D-1	Tandem duplication
Cotton A 12942	GaPIPLC4-1	Tandem duplication
Cotton A 12940	GaPIPLC4-4	Tandem duplication
Cotton A 21123	GaPIPLC4-2	Tandem duplication
Cotton A 21120	GaPIPLC4-3	Tandem duplication
Ghe05G09560	GhePIPLC4-1	Tandem duplication
Ghe05G09580	GhePIPLC4-2	Tandem duplication
Ghe09G13250	GhePIPLC4-3	Dispersed
Gorai.009G091700.1	GrPIPLC4-1	Tandem duplication
Gorai.009G091900.1	GrPIPLC4-2	Tandem duplication
Gorai.006G106400.1	GrPIPLC4-3	Dispersed

Table S3. Primers used in this work, Related to Figure 2, Figure 3, Figure 4, Figure 5, Figure 6.

Name	Sequences
	VIGS of *GhPIPLC2D* (endonuclease)
GhPIPLC2D	5'-GGACTAGTTTGGAGACATCCTGTTTTCACCT (*Spe*I)
	5'-TGGCGCGCCTTCCGTGAGTAATCGCAGCAT (*Asc*I)
	qRT-PCR analysis
GhACO1	5'-TAATCACAAATGGTAAATATA
	5'-TCGAACCTTGGCTCCTTGGC
GhACO2	5'-CAATCCTGGAAGTGATGCTGTT
	5'-CGAACCTCGGCTCCTTGTCT
GhACO3	5'-AAGAGTGTGGAGCACCGAGTC
	5'-CTTCTTTCTCCACCAACGCC
GhACO4	5'-GCCATCTCCCTGAATCAAACA
	5'-TTTTATCTGGGGTGGGGCAT
GhACS2	5'-AAAGCCTACGACAGCAGCCCTT
	5'-CATAACTATACGGTTCGGATCA
GhACS3	5'-ATGGGGAAAGTGAGGGGAGA
	5'-TGCCAACTCTAAAACCAGGGAAC
GhACS4	5'-GTGCCCGCAAAATGTCCA
	5'-GGAAAGAAGAACCTGGCGAAAC
GhACS6	5'-AAGTCGGTATCGGTTCGTTGAAGAGC
	5'-GGTGATTGAGGTATGGGAGAGTGAGG
GhACS10	5'-GTTATGACAGGGATGTAAAATGGC
	5'-TGTTCTTCTCTCTGGCAAAGTCTA
GhACS12	5'-CGCTTTATTCTACTTCCTCCAACTCT
	5'-TTTCTCAATCAAATCAAAACACAACC
GhPIPLC2A	5'-TTCAAAGAGTTCCCCTGTC
	5'-ATCATCTGTATCTTCCTC
GhPIPLC2D	5'- CTGAAGGAATTCCCGTCTC
	5'- CTTATCTCCATCGTCATCGAG
GhUBQ7	5'-GAAGGCATTCCACCTGACCAAC
	5'-CTTGACCTTCTTCTTCTTGTGCTTG